

Revision 1
MS #5732R

1
2
3
4
5
6
7
8
9
10
11 **A Mineralogical View of Apatitic Biomaterials**
12
13

14 Jill Dill Pasteris
15 Department of Earth and Planetary Sciences and
16 Institute for Materials Science and Engineering
17 Washington University in St. Louis
18 St. Louis, MO 63130-4899

19
20 pasteris@levee.wustl.edu
21
22
23
24
25
26
27
28
29

30 Revised version submitted to *American Mineralogist*
31 July 6, 2016
32
33
34
35
36
37
38
39
40
41

42 **Abstract**

43
44 Biomaterials are synthetic compounds and composites that replace or assist missing or
45 damaged tissue or organs. This review paper addresses calcium phosphate biomaterials that are
46 used as aids to or substitutes for bones and teeth. The viewpoint taken is that of mineralogists
47 and geochemists interested in (carbonated) hydroxylapatite, its range of compositions, the
48 conditions under which it can be synthesized, and how it is used as a biomaterial either alone or
49 in a composite. Somewhat counterintuitively, the goal of most medical or materials science
50 researchers in this field is to emulate the properties of bone and tooth, rather than the
51 hierarchically complex materials themselves. The absence of a directive to mimic biological
52 reality has permitted the development of a remarkable range of approaches to apatite synthesis
53 and post-synthesis processing. Multiple means of synthesis are described from low-temperature
54 aqueous precipitation, sol gel processes, and mechanosynthesis to high-temperature solid-state
55 reactions and sintering up to 1000 °C. The application of multiple analytical techniques to
56 characterize these apatitic, frequently nanocrystalline materials is discussed. An online
57 supplement details the specific physical and chemical forms in which synthetic apatite and
58 related calcium phosphate phases are used in biomaterials. The implications of this overview are
59 the enhanced recognition of the structurally-chemically accommodating nature of the apatite
60 phase, insight into the effects of synthesis techniques on the specific properties of minerals
61 (specifically apatite), and the importance of surface chemistry of apatite nanocrystals. The wide
62 range of synthesis techniques, types of analytical characterization, and applications to human
63 health associated with apatite are a non-geological demonstration of the power of mineralogy.
64 **Key words:** apatite, calcium phosphate, biomaterial, synthesis, bone, hydroxylapatite

89 **On-line Appendix (extensive)**

90

91

92

Introduction

93

94

95

96

97

98

99

100

101

102

103

The mineral component in bones and teeth is a highly carbonate-substituted, hydroxyl-deficient form of hydroxylapatite, $\text{Ca}_{10}(\text{PO}_4)_6(\text{OH})_2$. Bone and tooth are referred to biologically, geologically, and medically as biomineralized tissues or biomineralized materials. Intriguingly, however, they are not called "biomaterials." For the past few decades the latter word has been reserved for synthetic materials, including those that contain apatite, that temporarily or permanently replace biological tissues in humans or other animals (Williams 1987). In the words of Donglu Shi, "Biomaterials are artificial materials utilized to repair, assist, or replace damaged or missing tissue or organs...biomaterials can be classified into four different categories: metals, ceramics, polymers, and composites" (Shi 2006, p. 211). By this definition, synthetic forms of apatite and related calcium phosphate phases used to assist diseased or damaged bone or tooth tissue are ceramics or bioceramics.

104

105

106

107

108

109

110

111

The increasing need for such synthetic replacements arises not only from an expanding population, but also from the increasing percentage of senior citizens. For example, over 1,200,000 hip and knee surgeries/replacements occurred worldwide in 2013. Although apatitic materials are not strong enough to be used alone in load-bearing situations, such as the hip joint, they are critical as coatings on those stronger biomaterials, enhancers of new bone growth, and implants that do not support heavy loads. As illustrated in Figure 1, modern applications include treatments related to bone fractures, bone defects, cranio-maxillofacial reconstruction, dental implants, and spinal surgery (Hench and Wilson 1993; Dorozhkin 2010; Heimann 2013).

112 The types of natural apatite in the body and the biological responses to them are a
113 reflection of apatite's range of mineralogical-geochemical properties. Multiple papers over the
114 years have highlighted apatite's remarkable chemical-structural adaptability (Beever and
115 McIntyre 1946; Hughes et al. 1989; Elliott 1994; Kohn et al. 2002; White et al. 2005) as
116 revealed, for instance, by its ability to accept in solid solution up to half of the elements in the
117 periodic table (Pan and Fleet 2002; Hughes 2015), to retain or recover its crystallinity even under
118 assault from the decay of structurally incorporated radioactive elements such as uranium (Ewing
119 and Wang 2002; Harrison et al. 2002; Fox and Shuster 2014), to form in large-volume apatite
120 deposits through both low-temperature aqueous precipitation and high-temperature igneous
121 crystallization (Knudsen and Gunter 2002; Ihlen et al. 2014), and to constitute two distinctly
122 different types of biological apatite (Neuman and Neuman 1953; McConnell 1962; Young 1975;
123 LeGeros and LeGeros 1984; Daculsi et al. 1997; Baig et al. 1999; Elliott 2002; Wopenka and
124 Pasteris 2005; Glimcher 2006; Boivin 2007; Rey et al. 2009) in bone (typically with 5-8 wt%
125 CO_3^{2-} substitution) and tooth enamel (2-4 wt% CO_3). All of the above natural geological and
126 biological forms of apatite have been analyzed and interpreted by mineralogists and other
127 geoscientists, as well as by medical researchers and materials scientists. Likewise, medical
128 researchers and materials scientists, but few geoscientists, have described various biomedical
129 applications of apatite (cf. Heimann et al. 1997; Gross and Berndt 2002; short summary in
130 Rakovan and Pasteris 2015). The goal of the current paper is to describe and interpret apatitic
131 biomaterials from a mineralogical viewpoint and to indicate research directions to which
132 geoscientists could contribute.

133 **Criteria for bioapatite substitutes**

134 The two biological hard tissues that contain apatite, i.e., bones and teeth, exhibit many
135 differences as well as similarities. Specialized apatite biomaterials therefore are required
136 according to the anatomy and function of the original body tissue. Human bone comprises about
137 55-60 wt% apatite, ~30 wt% of the fibrous protein collagen I, and ~10-15 wt% water (Rogers
138 and Zioupos 1999). Bone is a nanocomposite in which bundles of collagen molecules, each
139 molecule less than 2 nm in diameter, form a scaffold that acts to nucleate and spatially organize
140 plate-like crystallites of carbonated apatite that are on the order of a couple of nanometers thick,
141 about 10-20 nm wide, and 20-50 nm long (Skinner 1987; Weiner and Wagner 1998; Rogers and
142 Zioupos 1999; Glimcher 2006; Alexander et al. 2012; Wagermaier et al. 2015). The mineral and
143 collagen are strongly bound to each other through (bio)chemical affinities that are still under
144 study (Sahai 2005; Landis and Jacquet 2013), but it is well known that this nanocomposite has a
145 strength and flexibility that are not possessed by either of its major constituent phases (Rogers
146 and Zioupos 1999; Currey 2006). Another important aspect of bone is that it undergoes periodic,
147 stress-induced replacement through a process called remodeling, in which specialized cells
148 (osteoclasts) dissolve small controlled volumes of mineral and collagen, which subsequently are
149 replaced (via osteoblasts) by new organized collagen and apatite (Glimcher 2006). Bone apatite
150 therefore must be sufficiently reactive in the acid produced by the osteoclasts to dissolve fully on
151 a relatively short time scale. At the millimeter scale of bone's hierarchical structure, one can
152 distinguish two types of material, i.e., (1) cortical bone – a very compact nanocomposite with
153 little porosity, which forms the external hard tissue in the outer portions of long bones like those
154 in the legs and arms and (2) trabecular bone – a very porous (up to 90 vol.%), spongy-looking
155 material in which the bone forms individual struts oriented in multiple directions, filling the ends

156 of long bones and the central regions of most bones, adjacent to the marrow cavity (Albright and
157 Skinner 1987; Glimcher 2006).

158 The anatomy of a tooth exhibits an even greater range of differences between its
159 mineralized sub-regions. The outermost surface of human teeth is covered and protected by a
160 form of bioapatite called enamel. Like bone, enamel is a nanocomposite of bioapatite and
161 organic components, but enamel differs from bone in multiple ways: it is > 95 wt% mineral
162 (apatite), with the remainder as water and proteins other than collagen; its crystallites are about
163 10 times larger in width and thickness than in bone, but 1000+ times longer. Whereas about 5-8
164 wt% CO_3^{2-} typically is substituted (mostly for PO_4^{3-}) in the apatite of bone mineral, enamel has
165 only about 2-4 wt% CO_3^{2-} (LeGeros and LeGeros 1984; Elliott 2002; Glimcher 2006). Enamel
166 also is not remodeled or replaced by the body. Beneath and grading into the enamel is the
167 dentin, which is a much more bone-like material in its collagen content and bioapatite mineral
168 chemistry, but dentin does not undergo remodeling (Carlson 1990). Molars are specialized
169 structures that can be placed under very large forces, i.e., up to 1.6 MPa pressure and over 350 N
170 force on portions of human molars during chewing. Such forces are not evenly distributed across
171 the tooth surface, illustrating the high strength and toughness required of enamel and its
172 biomaterial substitutes (Kohyama et al. 2004; Ferrario et al. 2004).

173 It might appear that, with more detailed information (which does exist) about the
174 biomineralized tissues above, the immediate goal of biomaterials research and the huge
175 biomaterials industry would be to synthesize exact replicas of the natural tissues. Although that
176 may be the ultimate goal, the multi-leveled hierarchical structures of teeth and bones presently
177 elude our synthesis capabilities. The more immediate and attainable goals have been to measure

178 and fully characterize the mechanical and chemical properties of natural biomineralized tissues
179 with the aim of simulating the latter's physical (especially mechanical) and chemical capabilities
180 during application, i.e., replicating functionality rather than material chemistry and structure.
181 Thus, we see references in the quotation above to biomaterials constructed from metals,
182 polymers, and ceramics, as well as statements in the literature heralding zirconia as the optimal
183 material for bone repair (Afzal 2014). The broader field of tissue engineering encompasses an
184 even more demanding goal in "the development of biomaterials that can promote regenerative
185 processes...transporting cell populations and therapeutic agents,...providing structural
186 scaffolding..." (Lee et al. 2014, p. 324).

187 **Biological constraints and terminology**

188 To be deemed successful, biomaterials must meet certain criteria and operate within
189 biologically necessary constraints, as illustrated in the terminology applied to these synthetic
190 materials.

191 **Biocompatible:** materials that can persist and function appropriately in the biological
192 environment without causing negative reactions in the biological tissue or the biomaterial. Three
193 important attributes of biocompatibility for biomaterials consideration are biochemical
194 compatibility (absence of toxicity, excessive inflammation, or carcinogenicity), biomechanical
195 compatibility (e.g., reasonable match in stiffness) with surrounding tissue, and biological
196 adhesion at the material-tissue contact (LeGeros 1988; Basu and Nath 2009). Some of the more
197 specific attributes of biocompatible materials are described by the following terms.

198 **Bioinert:** materials that do not induce bioadhesive bonding between the biomaterial and
199 tissue, e.g., bone. They also do not cause negative reactions, but they may induce non-adherent

200 capsules of scar tissue. Examples are alumina, zirconia, titania, and silicon nitride.

201 **Bioactive:** materials that can induce direct bio-adhesion at a tissue interface, i.e., through
202 chemical and biological bonding, typically early in the post-implantation period, without
203 intervening fibrous tissue. The phase that does form at the interface is carbonated
204 hydroxylapatite, similar to that in bone.

205 **Bioresorbable:** materials that are gradually dissolved and eventually totally replaced by
206 new tissue *in vivo*; ideally their resorption rate is very similar to the rate of tissue replacement *in*
207 *vivo* (Shi 2006; Basu and Nath 2009; Heimann 2013).

208 The following terms are specifically applicable to biomaterials used for the replacement
209 or reconstruction of bone.

210 **Osteoinduction:** ability to promote growth of new bone; stimulation of progenitor cells
211 leading to the formation of *osteoblasts* (bone-precipitating cells).

212 **Osteoconduction:** supporting the formation of bone on a material's surface, stimulating
213 ingrowth of surrounding bone, acting as a template or scaffold to guide the formation of new
214 bone, which requires interconnectivity of pores at appropriate spatial scales.

215 **Osteointegration:** chemical bonding directly with bone, without intervening fibrous
216 tissue; e.g., incorporation of an implant within bone to the extent that the implant is anchored,
217 physically stabilized, integrated into surrounding bone.

218 **Osteogenesis:** process of forming a layer of new bone (LeGeros et al. 2003, 2009;
219 Kretlow and Mikos 2007; Stevens 2008; Shepherd and Best 2011).

220 **The role and properties of biological apatite**

221 Apatite plays more than one role in vertebrate tissue. Not only is it the functionally

222 necessary hard phase in natural bone and tooth nanocomposites, but it also is the major chemical
223 reservoir of both calcium and phosphorus in the body. In case the biological/medical need arises
224 for more Ca or P to be available in body fluid, bone can be resorbed by osteoclasts to release
225 those elements (Glimcher 2006; Boskey 2007). Moreover, the specific composition of the
226 bioapatite, namely the carbonate:phosphate ratio, is both a monitor of and a buffer for the pH of
227 body fluid (Bushinsky et al. 2002). The fact that osteoclast and osteoblast cells are already
228 biologically programmed (Kanayama et al. 2011; Nakamura et al. 2016), respectively, to resorb
229 non-optimal calcium phosphate stores (e.g., old bone) and replace them with new, fully
230 functional bone also ensures apatite's enduring appearance among the constituents of
231 biomaterials.

232 There are multiple instances in which substitutes for natural bone and tooth materials are
233 required. The example of missing whole or partial teeth is the most straightforward to
234 understand. There is no biological mechanism for large-scale repair or replacement of the tooth,
235 in contrast to bone. The ability of bone to heal itself, however, is more limited than typically is
236 recognized. If a defect in the bone, for instance due to removal of a tumor, exceeds a critical size
237 (depending upon the animal in question), the body will not span the breach with woven bone as it
238 does for a simple fracture. Some bones with relatively small breaches also do not heal fully (i.e.,
239 nonunion bone defects), for instance, due to infection or insufficient blood flow to transport
240 needed ions and cells. Biomaterials are required to fill the breach and enable the bone to
241 recover. Although both the collagen and mineral component of the bone are required for optimal
242 regeneration, this review only addresses the mineral component.

243 One of the persistent misconceptions in the medical literature on bone is that

244 hydroxylapatite (HA), $\text{Ca}_{10}(\text{PO}_4)_6(\text{OH})_2$, is the mineral constituent in bones and teeth. This
245 oversimplification has made its way into the biomaterials literature, essentially ensuring that
246 stoichiometric HA is often selected for the mineral component in biomaterials. The actual
247 composition of bone mineral, however, is more like those shown in Skinner's (2005) compilation
248 or the formula $(\text{Ca}_{8.61-y}\text{Mg}_{0.2}\text{Na}_{0.42})[(\text{PO}_4)_{5.02-y}(\text{CO}_3)_{0.98}(\text{HPO}_4)_y](\text{OH})_{1.02-y} \cdot 1.5\text{H}_2\text{O}$, which is a
249 composition based on electron microprobe analyses of a hypermineralized (>95 wt% apatite)
250 bone (Li and Pasteris 2014). The subscripted "y" indicates an unknown but significant
251 concentration of $(\text{HPO}_4)^{2-}$ that will cause even greater depletion in OH and some additional
252 charge-balancing in the Ca-site. Note also the approximately 3 wt% of lattice-incorporated
253 molecular H_2O that, together with anions such as OH^- , resides in the channel sites (Yoder et al.
254 2012a; Pasteris et al. 2014). In any event, the strongly carbonated and hydrated phase that
255 comprises bone apatite is significantly different in composition from HA, which accounts for
256 bone apatite's higher solubility, smaller crystallite size, plate-like (rather than prismatic)
257 morphology, and incorporation of large amounts of both adsorbed and structural water in
258 distinction to stoichiometric HA. Its ability to accommodate variations in composition accounts
259 for much of apatite's biocompatibility and osteoconductivity (Heimann 2013).

260 **Some guiding principles for bioapatite-substituting materials**

261 The above comments on the currently dominant trends in the biomaterials industry should
262 not be interpreted to mean there is a dearth of research on how to simulate the true composition
263 of bioapatite or how to mimic the hierarchically organized nanocomposite of actual bone. For
264 multiple decades there have been research groups that experimentally have explored pathways to
265 creating carbonated apatites with all the pertinent properties of bone apatite (e.g., Neuman and

266 Neuman 1958; LeGeros et al. 1969, 1978; Termine 1972; Posner 1985; Rey et al. 1994, 1995,
267 2009; Daculsi et al. 1997; LeGeros 2008; Eichert et al. 2009; Tas 2014) and that have analyzed
268 in detail the structural and chemical properties of bone (e.g., Robinson 1955; Biltz and Pellegrino
269 1969; Zipkin 1970; Driessens and Verbeeck 1990; Veis 1993; Weiner and Wagner 1998; Elliott
270 2002; Glimcher 2006; Boskey 2007; Grynopas 2007; Xie and Nancollas 2010; Chen et al. 2011;
271 Landis and Jacquet 2013; Reznikov et al. 2014; Tao et al. 2015). There are also multiple
272 laboratories that are synthetically producing apatite-mineralized collagen (and other polymer)
273 constructs in an attempt to mimic the nano- to micro-meter scale hierarchy of bone (e.g., He et
274 al. 2003; Olszta et al. 2007; Deshpande and Beniash 2008; Nudelman et al. 2010, 2013; Liu et al.
275 2011, 2014; Habraken et al. 2016).

276 There is a clear need for bone and tooth substitutes. Bone material is second only to
277 blood as the most often transplanted tissue (Jones 2013). The first documented application of a
278 calcium phosphate (Ca-P) component to stimulate bone growth/regeneration is a 1920 article
279 describing experiments in which 1-ml aqueous aliquots of 5 wt% $\text{Ca}_3(\text{PO}_4)_2$ were injected into
280 surgically induced 6.3-mm gaps in dogs' legs. X-ray images of the affected legs showed
281 remarkably faster healing in the presence of just one such injection compared to untreated
282 controls (Albee and Morrison 1920). Almost one hundred years later, however, why do we still
283 focus on calcium phosphate/apatite? Why do we not exclusively choose stronger, lighter
284 substances with enhanced biomechanical functionality? Certainly, the inherent biocompatibility
285 of apatite is difficult to surpass, but Shepherd and Best (2011) identify apatite's prize
286 characteristic as its bioresorbability. The use of an appropriate composition of apatite for bone
287 replacement or reconstruction assures that the body does not have to permanently host a foreign

288 material, but rather that the original bone defect eventually becomes totally filled with and
289 strengthened by new, natural bone that has replaced a temporary, apatitic biomaterial. Habraken
290 et al. (2016) predict a bright future for Ca-P biomaterials as they continue to evolve.

291 The properties of apatite that must be emulated (either by the implanted materials or the
292 new bone that replaces the implants) are those imparted by nanometer-scale crystallite size,
293 ability to accommodate variations in composition, calcium deficiency compared to HA,
294 appreciable carbonate substitution in the structure, and atomic disorder that varies with the
295 concentration of carbonate. Experimental and clinical observations should guide the selection of
296 what compositions of apatite to use as bone substitutes and how to produce them. For instance,
297 in a comparison of responses to implant materials, carbonated HA was associated with increased
298 bone production over stoichiometric HA (Ellies et al. 1988; Rupani et al. 2012). In both in vitro
299 (Kanayama et al. 2011) and in vivo tests, carbonated apatite is more readily resorbed by
300 osteoclasts and replaced by new bone than is HA (Bang et al. 2014; Nakamura et al. 2016).

301 Whatever the calcium phosphate implant material, if its resorption rate is too slow,
302 growth of new bone is hindered. On the other hand, if the resorption rate is too fast, gaps
303 develop between the implant and the newly forming bone, possibly leading to mechanical failure
304 (Nilsson et al. 2013). For example, the stoichiometric HA phase does not dissolve passively over
305 time in the body; it must be biologically resorbed via osteoclast activity, i.e., through addition of
306 acid. Moreover, HA that is synthesized at or subsequently processed at elevated temperature is
307 highly crystalline and therefore remarkably un-bonelike. Such material can persist unresorbed in
308 the body for tens of years. Thus, the degree of crystallinity, which strongly affects solubility, is
309 a property of great significance in the formulation of apatite used as a biomaterial.

310 Much of the biocompatibility, bioactivity, and bioconductivity of bone arises from the
311 surface properties of its crystallites. The surfaces contain not only ions of the dominant elements
312 in the crystal lattice, but also minor ions such as Na^+ , K^+ , Mg^{2+} , and HPO_4^{2-} , that affect the
313 charge as well as chemical properties of the surface.

314 **Calcium-phosphate-based phases used in biomaterials and desired properties**

315 In the system $\text{CaO-P}_2\text{O}_5\text{-H}_2\text{O}$ are several calcium phosphate phases that are relevant
316 medically as biomaterials (see Table 1) and, to some extent, biologically in the formation of bone
317 and tooth (Skinner 1973; Brown 1992). These materials differ from each other chemically, e.g.,
318 in their Ca:P atomic ratios, the pH-sensitivity of their stabilities, and their solubilities, which are
319 of great importance. The solubility of Ca-P phases in water (see Figure 2) and in body fluid
320 (Johnsson and Nancollas 1992) is inversely proportional to their Ca:P ratio. Phases with a Ca:P
321 ratio less than 1 may not be implanted alone in the body, because they are either too soluble or
322 too acidic (Dorozhkin 2010). Ca-P phases also differ in the method by which they are
323 synthesized, either (1) by precipitation from an aqueous solution below 90 °C or (2) by chemical
324 synthesis or post-synthesis processing at high (400-1200 °C) temperature (Oliveira and Reis
325 2005). Many materials scientists still insist on high-temperature sintering of their biomimetically
326 produced materials, e.g., Na-substituted HA (Rupani et al. 2012: 700°C; Cho et al. 2013: 1100
327 °C). This sequence of materials handling seems counterintuitive. Although high-temperature
328 processing enhances the strength of such materials, as well as their crystallinity, it reduces their
329 bioactivity and bioresorption, thereby strongly decreasing the initial biomimetic character of the
330 product.

331 The crystalline Ca-P phases used most frequently in biomaterials are hydroxylapatite

332 (HA) and tricalcium phosphate (TCP), which exists in two polymorphic forms, α -TCP and β -
333 TCP (see Figure 3), where α -TCP (labeled on diagrams as α -C₃P) is the higher-temperature form
334 (see Table 1 for both sets of abbreviations). Only two Ca-P phases are stable in the presence of
335 body fluid or water at body temperature, and their stabilities are pH dependent (Fig. 2):
336 dicalcium phosphate dihydrate (DCPD), i.e., brushite (CaHPO₄•2H₂O; Ca:P = 1.0), stable at pH
337 < 4.2, and HA (Ca:P = 1.67), stable at pH > 4.2 (Riboud 1973; Kreidler and Hummel 1967;
338 Oliveira and Reis 2005; Shi 2006).

339 As documented in detail in Brown's (1992) study on the ternary system CaO-P₂O₅-H₂O
340 at 25 °C (see Figure 4), the phase relations in the compositional region of Ca:P = 1.0-1.67 are
341 more complex than typically has been acknowledged. For instance, there is a significant solid
342 solution field for "hydroxylapatite," extending from stoichiometric Ca₁₀(PO₄)₆(OH)₂ [Ca:P =
343 1.67] to so-called calcium-deficient apatite Ca₉(PO₄)₅(HPO₄)(OH) [Ca:P = 1.5]. Moreover, HA
344 dissolves congruently, whereas CaHPO₄ and CaHPO₄•2H₂O dissolve incongruently. Phase
345 relations in the ternary system at just about ten degrees higher than shown in Figure 4b are
346 directly applicable to the reaction(s) that produce natural bioapatite and those by which some
347 biomaterials are aqueously precipitated. The ternary system at 200 °C, as shown in Figure 4a,
348 represents phase relations at the low end of the sintering temperature range.

349 Although HA typically (however misguidedly) is recognized as the phase most similar to
350 bone mineral and has demonstrated itself to be strongly biocompatible and bioactive,
351 stoichiometric well crystalline HA both dissolves and precipitates at the slowest rate among all
352 the Ca-P bioceramic phases, making it bioactive, but essentially non-resorbable by passive
353 means in the body. In contrast, the much more soluble TCP (Fig. 2) has a dissolution rate so

354 high that it exceeds that of the regeneration of bone tissue. Application of TCP therefore is
355 typically in the form of a mixture of TCP and HA (LeGeros et al. 2003; Shi 2006).

356 Apatite has lackluster mechanical properties (see Table 2). For this reason, monolithic
357 constructs of pure HA and other HA bioceramics are not used as load-bearing biomaterials, but
358 rather as micro- and nano-particulate powders, coatings, and porous scaffolds (Shi 2006). HA,
359 however, works effectively in composites with other crystalline materials (e.g., Al₂O₃ or ZrO₂),
360 with natural (e.g., collagen) and synthetic (e.g., polyethylene, polylactic acid) polymers, and --
361 most importantly -- as a coating on implants such as hip and knee replacements (Nath and Basu
362 2009; LeGeros et al. 2009; Heimann 2013, 2016).

363

364 **Synthesis Methods of Apatite for Use in Biomaterials**

365 The synthesis technique determines not only which Ca-P phase is produced, but also the
366 properties of that phase, such as solubility, morphology, porosity, surface activity, and crystallite
367 size. Somewhat counterintuitively, most apatite in biomaterials either has been synthesized at or
368 subsequently processed (i.e., sintered) at high temperature (400-1200 °C), presumably to produce
369 a more stiff, easily handled material. The most common Ca-P phase in biomaterials is
370 stoichiometric HA. The first Ca-P phases used as biomaterials were HA and β-TCP, both
371 synthesized at high temperature. As mentioned above, they often are used together as what is
372 called biphasic calcium phosphates, BCP (LeGeros et al. 2003; Daculsi et al. 2009, 2010), due to
373 their different rates of resorption (Eichert et al. 2009). Hench (1998) provides detailed
374 discussions of clinical applications of individual biomaterials. The current state of knowledge
375 about the structure and composition of high-temperature, high-pressure carbonated

376 hydroxylapatite is documented and discussed in Fleet (2015). Additional, more specific
377 information on the physical forms in which Ca-P materials are manufactured for biomedical use
378 and some of the biological responses to their use appears in the online supplement.¹

379

380 ¹ Deposit item AM-....., Supplementary Material. Deposit items are free to all readers and found
381 on the MSA web site, via the specific issue's Table of Contents (go to
382 <http://www.minsocam.org/MSA/AmMin/TOC/>).

383

384 There is, however, increasing interest in low-temperature (room temperature to about 400
385 °C) synthesis techniques that can be tailored to produce a range of chemical compositions (e.g.,
386 carbonate concentration), lead to a more biomimetic product, and save energy (Eichert et al.
387 2009). Such low-temperature materials tend not to be HA but rather non-stoichiometric and Ca-
388 deficient apatite, as are bone crystallites. Their Ca-deficiency can be controlled by the
389 temperature and pH of precipitation, mainly through the equilibrium concentration of HPO_4^{2-} in
390 the solution.

391 The above interest in more biomimetic synthesis techniques is consonant with current
392 emphasis on the bioactivity and osteostimulation properties of apatitic biomaterials. There is
393 increasing recognition of the importance of detailed physical and compositional features of the
394 materials synthesized. Physically, those mesenchymal stem cells (from bone marrow) that
395 differentiate into bioapatite-precipitating osteoblasts are sensitive to micrometer- and nanometer-
396 scale topography on biomaterials. Their cell differentiation occurs more rapidly on a surface of
397 randomly distributed pits than on one with a highly ordered array of such pits (Stevens 2008).

398 This response suggests that an atomically disordered apatite might be biologically favored.
399 Compositionally, recognition that Mg^{2+} (up to about 0.75 wt%) and $(\text{CO}_3)^{2-}$ (up to ~7 wt%) are
400 significant components in bone apatite has provided pathways to increased tailoring of the
401 properties of apatite synthesized for biomaterials (Suchanek et al. 2004; Nakamura et al. 2016).
402 As briefly described below, the solid-state and wet-chemical techniques used to synthesize
403 apatite strongly affect the mineral's internal and surface properties.

404 **Solid-state reactions**

405 Stoichiometric HA can be formed at elevated temperatures by reacting $\text{Ca}(\text{OH})_2$ with
406 either CaHPO_4 or $\text{Ca}_3(\text{PO}_4)_2$ accompanied by release of excess H_2O . The raw materials typically
407 are ground, mixed, compressed, and then sintered at $> 950\text{ }^\circ\text{C}$ to enhance ion diffusion.

408 Substituted apatites, such as with Sr for Ca and F for OH substitutions, can be created with the
409 addition of other reagents to the above. Ion diffusion in the solid state leads to well crystalline
410 HA. Varying the ratio of the reactants can lead to biphasic products such as TCP + HA, which
411 are desired end-products for certain uses (LeGeros and LeGeros 1993; Shi 2006; Shepherd and
412 Best 2011).

413 **Plasma-sprayed hydroxylapatite coatings**

414 Biomaterials must fulfill the demands of both biocompatibility and appropriate
415 mechanical properties. To meet the demands for strength, as in the replacement of the total hip
416 joint or tooth socket, a metal (e.,g., steel, titanium) implant may be called for. Metals, however,
417 are not osteoinductive or osteoconductive. A transitional phase is needed to stably bond with the
418 metallic implant, as well as to induce bonding with the existing adjacent and newly forming
419 bone. Apatitic coatings are ideal for this purpose, as shown by the 2- to 7-fold increase in

420 interfacial bond strength of porous Ti when plasma-sprayed with apatite (Hench 1998). Plasma-
421 sprayed HA coatings, as have been so effective for hip replacements and other metal implants,
422 constitute the most widespread application of hydroxylapatite in biomaterials.

423 Apatitic coatings can be deposited at low (<40 °C) or high (many hundred degrees
424 Celsius) temperatures. For plasma-spraying, the most common high-temperature process, HA
425 particles (feedstock) are melted and projected at high velocity by a plasma (e.g., of argon) at
426 5000-20,000 °C. The molten droplets are flash quenched as they splat onto the surface of the
427 target metal (Carayon and Lacout 2003; Shi 2006; Dorozhkin 2012b; Heimann 2013, 2016).

428 Among the challenges to the functionality of plasma-sprayed HA are its possible non-
429 uniformity in thickness and coverage, and its crystallinity. The high temperature imparted by the
430 plasma to the surface of an implant also can produce problems (Oliveira and Reis 2005). More
431 details on the plasma-spraying techniques are available in the appendix.

432 **Mechanosynthesis**

433 Mechanosynthesis (also called mechanochemical synthesis) is typically a solvent-free
434 technique for the synthesis of nanoparticulate compounds. For the purpose of combining metals
435 or oxides to form compounds, mechanochemical synthesis appears to have become an accepted technique
436 early in the 1990s (Sepelak et al. 2012). Only in about the past 15 years (Boudeville et al. 2001)
437 has it been applied to Ca-P compounds, especially for production of biomaterials. The technique
438 involves placing a few compositionally simple, solid components (e.g., oxides, salts) into a high-
439 energy ball mill, as of the planetary ball mill type, and operating the system for periods of a few
440 minutes to hours. This process produces a homogeneous, nanocrystalline new compound whose
441 stoichiometry exactly reflects the ratios of the reactants (Chaikina et al. 2004; Mochales et al.

442 2011).

443 Activation of the reaction at room temperature occurs mechanically when the dry
444 components are impacted between two metal/ceramic balls or between one ball and the walls of
445 the mill. Among the common reactants to produce Ca-P phases are acid phosphates (as
446 discussed in the next section), whose reactions generate water. This internally produced water is
447 important to the mechanochemical synthesis and to the generation of more ductile particles
448 compared to the original brittle constituents (Chaikina et al. 2004; Fahami et al. 2015). Ca-P
449 samples produced this way have broader XRD peaks (indicative of smaller grain size) than
450 compositionally similar phases produced by thermal synthesis, which is attributed both to their
451 low synthesis temperature and mechanically induced defects. Mechanochemically synthesized
452 Ca-P materials have a particle size on the order of 15-20 nm, but the particles typically aggregate
453 into granules up to 100 nm. The degree of (non-)stoichiometry and chemical substitution (as by
454 CO₃, Na, K, Zn) in various apatitic products is controlled by the choice and ratio of the reactants
455 (Chaikina et al. 2004; Suchanek et al. 2004; Mochales et al. 2011). Variations on the dry
456 mechanochemical synthesis method include the preparation of powder-water slurries of the
457 reactants, which are then mixed and processed in a ball mill, a technique referred to as
458 mechanochemical-hydrothermal synthesis. Although instantaneous temperatures may be
459 elevated at the point of impact in the ball mills, thermocouple measurements during a
460 mechanochemical-hydrothermal experiment were close to room temperature (Suchanek et al.
461 2004). The most significant concern is possible contamination of the product by particles
462 abraded from the ball mill materials.

463 **Low-temperature, wet-chemical synthesis techniques**

464 Water is the solvent/reactant either for (1) chemical precipitation induced by mixing of
465 Ca- and P-bearing solutions or for (2) hydrolysis of a single starting phase. Precipitation
466 reactions at 25-95 °C and 1 atm can involve any of several pairs of soluble salts of calcium and
467 phosphorus, such as $\text{CaCl}_2 + (\text{NH}_4)_2\text{HPO}_4$ or $\text{Ca}(\text{NO}_3)_2 + (\text{NH}_4)_2\text{HPO}_4$. One of the earliest
468 procedures was to create an aqueous suspension of $\text{Ca}(\text{OH})_2$ into which H_3PO_4 was added
469 dropwise: $10\text{Ca}(\text{OH})_2 + 3\text{H}_3\text{PO}_4 \rightarrow \text{Ca}_{10}(\text{PO}_4)_6(\text{OH})_2 + \text{X}$. Ammonium hydroxide was added to
470 the solution to retain a strongly basic pH, helping to assure that the HA precipitate was
471 stoichiometric (LeGeros and LeGeros 1993). An alternative method was reaction of calcium
472 nitrate and ammonium hydrogen phosphate, with ammonium hydroxide again added to assure
473 high pH: $10\text{Ca}(\text{NO}_3)_2 + 6(\text{NH}_4)_2\text{HPO}_4 + 2\text{NH}_4\text{OH} \rightarrow \text{Ca}_{10}(\text{PO}_4)_6(\text{OH})_2 + \text{Y}$. Calcium acetate
474 often was preferred over calcium chloride or nitrate, to avoid incorporation of the latter two
475 anions in the apatite structure (LeGeros and LeGeros 1993). For the same reason, ammonium,
476 rather than sodium, hydrogen phosphate was preferred. A soluble carbonate such as NaHCO_3
477 can be added, and the $\text{CO}_3:\text{PO}_4$ ratio of the solution can be used to control the degree of
478 carbonate substitution in the apatite. Likewise, substituents for Ca (e.g., Mg, Sr), OH (e.g., F, Cl,
479 Br), and non-carbonate substituents for PO_4 (e.g., VO_4 , BO_3) can be introduced during synthesis
480 (e.g., LeGeros and LeGeros 1993; Yoder et al. 2012b; Goldenberg et al. 2015).

481 If HA is the desired product, the disadvantages of the above synthesis route are its typical
482 formation of non-stoichiometric apatite and its contamination with CO_3 , HPO_4 , and other ions
483 (e.g., K, Na, NO_3 , Cl) that were present in the reactants (Wilson et al. 2006b; Shi 2006; Shepherd
484 and Best 2011). An alternative to mixing two solutions is to use a single solution of chemically
485 simulated body fluid, SBF, in some cases at concentrations higher than physiological (such as

486 1.5xSBF or 2xSBF) in order to stimulate precipitation (e.g., Tas 2014). Apatite precipitation
487 from 1.0xSBF solutions is a reminder that body fluid actually is supersaturated with respect to
488 bioapatite, which is prevented from precipitating by the presence of biomolecular nucleation
489 inhibitors, except where desired (Menanteau et al. 1982; Pasteris et al. 2008; Talmage and
490 Mobley 2009; Drouet 2013; Landis and Jacquet 2013).

491 Synthesis solutions must be pH-buffered to assure that apatite, e.g., not brushite, is the
492 equilibrium product. Ion concentrations of the two reacting solutions typically are chosen to
493 cause high degrees of supersaturation with respect to an apatite phase upon mixing. The
494 coupling of supersaturation with the low temperature (<100 °C) of the solutions does not
495 encourage equilibration in the system. There is evidence that an intermediate phase, such as
496 octacalcium phosphate, often forms before and may affect the stoichiometry of the final apatite
497 product (Brown et al. 1991; Borkiewicz et al. 2010).

498 The second type of low-temperature aqueous reaction that will produce an apatitic
499 product involves hydrolysis of acid Ca-P phases that are not stable in water. Among the possible
500 starting phases are DCPD, DCP, TCP, and OCP (see Table 1), which can produce Ca-deficient
501 apatite powders (Shi 2006). Depending on the desired composition of the apatitic product,
502 aqueous solutions of chloride, fluoride, carbonate, or hydroxides of sodium, potassium, or
503 ammonium can be used. Hydrolysis of TTCP, α -TCP, β -TCP, or amorphous calcium phosphate
504 (ACP) also yields calcium-deficient apatite. To create a less Ca-deficient apatite and thereby
505 decrease the amount of TCP produced during sintering, appropriate amounts of Ca(OH)₂ can be
506 added to the synthesis solutions (LeGeros and LeGeros 1993).

507 In contrast to high-temperature dry reactions, aqueous methods involving either reaction-

508 precipitation or hydrolysis save energy and produce non-stoichiometric apatite, whose advantage
509 is higher solubility and more biomimetic character than HA. By decreasing the solution
510 temperature and by increasing the degree of carbonation, the size of the precipitate grains can be
511 decreased, while also producing a higher surface-area-to-volume ratio. The effects of
512 substituting other ions are detailed in LeGeros et al. (2009). Another important example of low-
513 temperature aqueous formation of apatite is in the self-setting pastes (when mixed with water)
514 known as bone cements. These are discussed in the online supplement.

515 **Sol-gel processes**

516 Sol-gel processes at room temperature can be used to create either bioactive glass or
517 crystalline HA. In the making of a glass, a silica-rich solution (such as tetraethyl orthosilicate)
518 with the desired precursor components (typically Ca, P, and Si, but P can be absent) is reacted
519 with water under either acidic or basic conditions. Polymerization occurs through hydrolysis,
520 and a sol of spherical nanoparticles forms. Specific solution conditions cause the nanoparticles
521 to coalesce and bond together to form a gel. This aqueous network of covalently bonded silica
522 tetrahedra undergoes drying and subsequent heating to $> 600\text{ }^{\circ}\text{C}$, which forms a nanoporous
523 glass (Jones 2013). The sol-gel process of forming bioactive glass permits a wider range in SiO_2
524 concentrations and higher chemical purity than would melting. The pH of the original solution is
525 very important to the degree of crystallinity of the product after heating, e.g., pH = 9 may yield
526 an amorphous phase (Dorozhkin 2012a), whereas an initial pH of 11.5 can yield crystalline
527 products (Luz and Mano 2011).

528 Synthesis of crystalline HA via a sol-gel process begins with the mixing of calcium
529 nitrate and a phosphate compound (in the exact molar ratio of Ca:P = 1.67), dissolved in ethanol

530 at temperatures < 100 °C, to produce an amorphous Ca-P precipitate. Subsequent sintering at
531 several hundred degrees Celsius produces a single-phase powder of stoichiometric HA that does
532 not break down until temperatures above 1200 °C, indicating high purity and exact
533 stoichiometry. Particle sizes of the phase-pure HA range down to less than 10 nm (Kuriakose et
534 al. 2004; Kim and Kumta 2004). Compared to other techniques to synthesize HA, e.g., aqueous
535 precipitation, hydrothermal formation, and electrodeposition, the sol-gel method offers the
536 benefits of low temperatures, high purity, and the ability to produce nanoparticles without
537 grinding. Allowing the precipitate to age for a sufficient time (48 hrs. in one study) is necessary
538 in order to assure phase purity, e.g., no detectable TCP (Bakan et al. 2013).

539 **Hydrothermal methods**

540 Aqueous solutions in pressure vessels are taken above 100 °C at elevated pressures in
541 various types of chemical systems. For instance, TCP or TTCP in the presence of Ca(OH)₂ can
542 be converted readily to HA by hydrothermal reaction at 275 °C and steam pressure of about 80
543 MPa (LeGeros and LeGeros 1993). Continuous hydrothermal flow synthesis works well to
544 create HA nanoparticles, as well as HA with controlled degrees of carbonate or silica
545 substitution. Chaudhry et al. (2012) produced the latter two types of substituted apatites at 400
546 °C and 24 MPa, both of which are more bioactive than pure HA.

547 Hydrothermal techniques also can be used to transform calcium carbonate to (carbonated)
548 HA, especially to make use of the inherent porosity of carbonate-biomineralized coral and
549 cuttlebones in the production of porous scaffolds for new bone growth. The typical conversion
550 reaction used is CaCO₃ + CaHPO₄ or (NH₄)₂HPO₄ to produce Ca₁₀(PO₄)₆(OH)₂.

551 Calcium carbonate-biomineralized materials are selected for their pore sizes, 3-D

552 microstructure, and surface nanomorphology. Hydrothermal solutions at temperatures of about
553 270 °C and pressures of about 85 MPa are used to transform corals into HA with an
554 interconnected porosity of about 65 vol%, exactly mimicking that of the coral (Gross and Berndt
555 2002; Shi 2006). In another example, cuttlebone, the internal aragonite skeleton of the cuttlefish,
556 has a microstructure much like that of trabecular/spongy bone. The organic material of the
557 cuttlebone is chemically removed through bleaching, which also eliminates health concerns. The
558 above reaction is then carried out at 180 °C in a Teflon-lined, stainless steel reactor. The
559 resultant porous apatite scaffold has a high protein-adsorption rate; it can induce bone formation
560 on its surfaces even without the addition of bone growth factors and living cells, which otherwise
561 could cause medical problems (Hongmin et al. 2015). Such phosphate-pseudomorphed
562 constructs are almost as successful as autografts in inducing new bone growth, but they eliminate
563 the worries of permanent damage to the patient at the site from which bone material would have
564 been removed for autografting.

565 Hydrothermal conversion of carbonate-biomaterialized materials also enables facile
566 production of the more (cf. HA) biomimetic carbonated apatite. Low-porosity blocks of
567 carbonated hydroxylapatite (CHA) also can be produced from blocks of gypsum ($\text{CaSO}_4 \cdot 2\text{H}_2\text{O}$)
568 or calcite by hydrothermal conversion using $(\text{NH}_4)_2\text{HPO}_4$ or Na_2HPO_4 (LeGeros et al. 2009).

569 Combined "mechanochemical-hydrothermal" synthesis (see "mechanosynthesis" section
570 above) can be used to produce Mg- and CO_3 -bearing HA (Suchanek et al. 2004). The
571 component powders of $\text{Ca}(\text{OH})_2$, MgCO_3 , and $(\text{NH}_4)_2\text{HPO}_4$ are placed in a small amount of
572 water and ground in a multi-ring media mill. The as-formed Ca-P material is X-ray amorphous
573 and relatively homogeneous. Heat treatment can follow at several hundred degrees Celsius to

574 produce Mg-CO₃-bearing apatites of compositions controlled by the initial bulk chemistry, the
575 temperature of subsequent heating, and the (low) solubility of Mg in HA (Suchanek et al. 2004).

576 **Fabrication of porous, apatitic biomaterials**

577 For high-temperature processing that produces porous material, powders of bioceramic
578 particles can be mixed with organic components, such as starch or polymethylmethacrylate. The
579 mixture is compressed into the desired shape and then heated to burn out the polymer
580 component. Higher-temperature sintering of the bioceramic often follows, producing a material
581 with up to 70% porosity (Shi 2006). Alternatively, a slurry of bioceramic particles <100 μm
582 diameter, a water-soluble compound of high molecular weight (e.g., a cellulose derivative), and a
583 fatty acid that acts as a non-ionic surface-active agent are all vigorously stirred at a temperature <
584 20 °C. The slurry is frothed by addition of a non-reactive gas. The material forms a gel, which
585 is dried at < 100 °C, degreased at much higher temperatures, and then sintered at ≥1000 °C.
586 Higher temperatures yield higher-strength materials. The products can have up to 80% porosity
587 with pore sizes of 5 to 1500 μm (Naqshbandi et al. 2013). Numerous procedures to form porous
588 biomaterials have been patented, including freeze casting and use of polymer sponges, as
589 described by Naqshbandi et al. (2013) and compared via extensive illustrations and tables.

590 Lower-temperature processes include adding soluble particles such as salt or sugar to
591 mixtures of Ca-P phases that react to form HA in the presence of water (e.g., TTCP + CaHPO₄
592 → HA). The soluble particles dissolve leaving a porous solid behind. Most such porous
593 bioceramics have very weak biomechanical properties, but these increase markedly with
594 ingrowth of new bone into the pores (Shi 2006).

595 **Compacting and sintering of nanocrystalline apatites**

596 The level of biocompatibility of Ca-P bioceramic materials is highest when the material
597 is nanocrystalline and carbonated, i.e., biomimetic, but these attributes also create the least
598 favorable mechanical properties. To counter the latter problem, Ca-P ceramics typically are
599 sintered at 1000-1200 °C. Particle coalescence begins below 1000 °C, but actual densification
600 increases with temperature above 1000 °C. Hydroxylapatite, however, becomes unstable above
601 1250-1300 °C depending on its exact composition (Dorozhkin 2010) and on the water pressure
602 of the system (cf. Fig. 3). Sintering causes the following chemical changes in the bioceramic:
603 release, as gases, of molecular water (adsorbed and structurally incorporated) and carbonate, as
604 well as volatiles remaining from the synthesis reactions; increase in crystal size and decrease in
605 surface area; transformation of any HPO_4^{2-} component of the apatite into $\text{P}_2\text{O}_7^{4-}$ accompanied by
606 the release of H_2O ; the apatite becomes more stoichiometric in composition, including filling of
607 OH-vacancies in the channel sites by OH^- ions derived from the released H_2O ; and the apatite
608 gains toughness and mechanical strength (Dorozhkin 2010; Pasteris et al. 2014). In the many
609 ways listed above, Ca-P bioceramics that are constructed ex situ and inserted into the body,
610 differ from natural biological hard tissue.

611 Low-temperature consolidation processes are a compromise, in which the inherent
612 properties of the hydration layer of HA nanoparticles are better preserved. Uniaxial compression
613 below 200 °C causes crystal-crystal interactions that, in conjunction with ion mobility in the
614 hydrated surface layers, produce a more compact and ceramic-like material with enhanced
615 mechanical properties that can approach the values for materials sintered at much higher
616 temperature (Drouet et al. 2009).

617 Dorozhkin (2010) documents the values of specific mechanical properties in HA

618 bioceramics (cf. Table 2), comparing them to those of bone and tooth enamel. Fracture
619 toughness of Ca-P bioceramics is less than half of that for human bone, whereas mechanical
620 strength increases with the Ca:P ratio of the material up to a maximum at a Ca:P ratio of 1.67
621 (HA). The Young's modulus of dense HA bioceramics is 35-120 GPa compared to ~18-22 GPa
622 for cortical bone. It is this brittleness of HA bioceramics that precludes their use as load-bearing
623 implants (Dorozhkin 2010).

624 **Synthesis of substituted apatites, particularly by SiO_4^{4-}**

625 Atomic substitutions in the apatite structure, such as Sr^{2+} for Ca^{2+} , F^- for OH^- , and CO_3^{2-}
626 for PO_4^{3-} , can be produced via modest changes to the composition of the reactants in the
627 synthesis. In biomaterials, such ions typically are incorporated to better mimic the composition
628 of natural bone (e.g., CO_3^{2-}) or for therapeutic applications (e.g., Sr^{2+} to address osteoporosis).
629 Because modern calcium phosphate bioceramics typically are designed to be resorbed, their
630 formulation also provides the opportunity to include elements such as Sr^{2+} , Zn^{2+} , or Si^{4+} that can
631 assist in bone healing when they are released during dissolution (Salinas et al. 2013). In aqueous
632 syntheses, for instance, soluble metal nitrates could be used to introduce cations, whereas soluble
633 metal halides could be used to introduce anions for the channel site (see citations in Goldenberg
634 et al. (2015) for methods of specific ion substitutions).

635 In addition to the carbonated apatites discussed in several sections of this paper, only one
636 other substitution of significance to biomaterials will be described, i.e., that of silicate. Silicon is
637 known to be a trace component in bone mineral (Quelch et al. 1983) and collagen and to be
638 important to the healthy formation of both (Jugdaohsingh 2007; Mostafa et al. 2011). The
639 formulation and proposed application of silicate-substituted apatites as biomaterials follows from

640 the above observations as well as from the widely recognized success of silicate-based bioactive
641 glasses (see online supplement) and the documented substitution in geological apatites of SiO_4^{4-}
642 for PO_4^{3-} (McConnell 1937; Pan and Fleet 2002). It is also possible to substitute small
643 concentrations of silicon in TCP, reported as $\text{Ca}_3(\text{P}_{0.9}\text{Si}_{0.1}\text{O}_{3.95})_2$ (Reid et al. 2005). Si-substituted
644 apatites typically are precipitated from aqueous solutions, in which silicon tetra-acetate
645 $[\text{Si}(\text{COOCH}_3)_4]$ or silicon tetra-ethyl orthosilicate $[\text{Si}(\text{OCH}_2\text{CH}_3)_4]$, TEOS] is a reactant
646 (Chaudhry et al. 2012; Bang et al. 2014) or to which sodium silicate has been added (Mostafa et
647 al. 2011). One alternative method is to precipitate a Ca-P phase aqueously, mix it with fumed
648 silica particles, and subsequently sinter the mixture at about 1000 °C (Reid et al. 2005).

649 Many groups have worked on the formulation and characterization of silicate-substituted
650 hydroxylapatite (Si-HA), but some of the mineralogically most interesting work has been done
651 on multi-substituted HA, e.g., by CO_3^{2-} and SiO_4^{4-} (Bang et al. 2014) and by Na^+ , CO_3^{2-} , and
652 SiO_4^{4-} (Mostafa et al. 2011). The latter two studies also made excellent use of analytical
653 techniques (see next section) that were well selected to characterize the resultant apatitic
654 materials. Their results on Si-HA confirmed those of other researchers, namely that SiO_4^{4-}
655 substitution causes a decrease in crystallite size and degree of crystallinity in the apatite.

656 Mostafa et al. (2011) and Bang et al. (2014) both determined from experiments that
657 doubly substituted Si- CO_3 -HA powders had an even smaller particle size and crystallite size than
658 their CO_3 -HA counterparts. Compositional analyses (especially for Ca:P atomic ratio) strongly
659 indicated that CO_3^{2-} and SiO_4^{4-} both substitute primarily for PO_4^{3-} , that is, they compete for the
660 PO_4^{3-} site. Although the two research groups observed different upper bounds on the
661 concentration of SiO_4^{4-} that was structurally incorporated (which appears to depend on the

662 concentration of incorporated CO_3^{2-} -- different in the two studies), both groups detected the
663 eventual formation of an apparently amorphous and incipiently polymerized siliceous coating on
664 the samples. Bang et al. (2014) additionally tested the response of mechanical properties to the
665 substitutions. When SiO_4^{4-} was added to CO_3^{2-} as a substituent, the sintered apatites were denser
666 and also stronger under tension than CO_3 -HA. Moreover, the incorporation of SiO_4^{4-} increased
667 solubility over that of CO_3 -HA alone (Bang et al. 2014). Mostafa et al. (2011) provided details
668 on the mechanisms of charge balance due to substitution of PO_4^{3-} by CO_3^{2-} and/or SiO_4^{4-} . The
669 mechanisms changed according to the concentration of SiO_4^{4-} , which reached at least 2.23 wt%
670 Si incorporation in the lattice; the CO_3^{2-} concentration rose as SiO_4^{4-} did (Mostafa et al. 2011).
671 In their Si-HA samples, Chaudhry et al. (2012) reported an upper bound of 1.1 wt% Si.

672 In recognition of the known importance of Mg in the development of healthy bone and its
673 recorded concentration of 0.12-1.07 wt% MgO in natural bone (Skinner 2005; Li and Pasteris
674 2014), Sprio et al. (2008) studied the effects on HA of substitution by Mg^{2+} , CO_3^{2-} , and SiO_4^{4-} .
675 They interpreted from their solubility experiments that the apparent incongruent dissolution of
676 multi-substituted apatite probably reflects the non-stoichiometric composition and concentration
677 of ions in the hydration layer on the individual crystallites. As above, Sprio et al. (2008) also
678 found evidence that CO_3^{2-} and SiO_4^{4-} competed for occupation of the PO_4^{3-} site, but unlike in
679 later studies (Mostafa et al. 2011; Chaudhry et al. 2012; Bang et al. 2014), they reported a
680 combined $\text{CO}_3^{2-} + \text{SiO}_4^{4-}$ concentration beyond which the Ca-P product was X-ray amorphous.
681 Concentrations of up to 2.4 wt% Si were stably incorporated in carbonated (2.4 wt% CO_3) HA.
682 Incorporation of approximately biological concentrations of all three substituents were attained
683 in some of the experiments (Sprio et al. 2008).

684 Si-HA has been tested in vivo against other biomaterials, including TCP and calcium
685 sulfate. Si-HA showed itself to be strongly bioactive, e.g., resorbed biologically by osteoclasts
686 rather than undergoing passive dissolution. Its resorption rate, analogously to that of CO₃-HA, is
687 well synchronized with the rate of new bone deposition, allowing Si-HA scaffolds to retain their
688 ability to support the bone structures surrounding them (Hing et al. 2007).

689

690 **Characterization of Apatite for Use in Biomaterials**

691 “Although apatites are among the most stable and most easily formed calcium
692 phosphates, their composition, and crystal structure are still the object of intense research” (Rey
693 et al. 2007b, p. 198). Not all “apatites” are the same, and not every phase comprising calcium
694 and phosphate is an apatite. Quality control on every Ca-P bioceramic requires phase
695 identification and determination of basic physical-chemical properties (e.g., particle size,
696 porosity, density, chemistry). More detailed compositional and structural data than the above
697 would be needed to provide insights into a specific Ca-P’s level of bioactivity, the mechanism(s)
698 of its interaction with tissues, and its ability to stimulate osteogenesis at the cellular level. Data
699 continue to be compiled on the physical-chemical characteristics of these bioceramics in
700 conjunction with their responses in vitro and in vivo to simulated or actual physiological
701 conditions (both chemical and cellular), as exemplified below.

702 There are two main reasons behind the need for multi-instrument, detailed analyses of
703 synthetic Ca-P biomaterials. Firstly, there are so many different synthesis pathways and recipes
704 for the fabrication of Ca-P biomaterials that one should not assume all products with the same
705 name, e.g., "hydroxyapatite," have the same properties. For instance, there are concerns about

706 incorporation of impurities – not externally derived contaminants, but rather retention of the
707 additional ions that were introduced into the synthesis solution from reactant compounds, e.g.,
708 Na^+ , Cl^- , and NH_4^+ (Koutsopoulos 2002). Secondly, apatite's lattice is so accommodating that
709 even small differences in temperature of formation, time for maturation in the precipitating
710 solution, post-precipitation storage environment, etc. could induce chemical and/or physical
711 differences among aliquots of "the same" kind of apatite (Vandecandelaere et al. 2012).

712 Mineralogists and materials scientists are well aware of the many tools available for bulk
713 and point analysis of the chemistry and structure of crystalline and non-crystalline materials.
714 This section therefore is limited to highlighting the analysis of some properties of nanocrystalline
715 apatite and its end-products (e.g., after heat-treatment) that are important to their functionality as
716 biomaterials, e.g., phase identity, degree of crystallinity, crystallite and particle size, particle
717 shape, chemical composition, solubility, and reaction with biological tissue and fluids (Shi
718 2006).

719 The nanometer scale, low degree of crystallinity, and reactive-metastable nature of
720 biomimetic apatite (often the raw or "green" product of reaction) make it difficult to characterize
721 reproducibly. For instance, one of the most important controls on the bioactivity of
722 nanocrystalline apatite is its surficial hydration layer, yet this is one of the most challenging
723 features to document. This ion-rich coating on apatite nanoparticles enhances the mobility of its
724 entrained ions as well as their transfer from the coating to the underlying crystal lattice (Neuman
725 and Neuman 1958; Rey et al. 2007a; Bertinetti et al. 2009; Eichert et al. 2009). The presence of
726 a surficial, hydrated, ion-rich layer also makes it difficult to distinguish how much carbonate is
727 within the apatite lattice compared to how much is in the hydration layer – a parameter that

728 affects bioactivity and therefore should be documented, but is extremely difficult to measure.
729 Another analytical challenge is determining how much HPO_4^{2-} (which, together with CO_3^{2-} ,
730 substitutes in the PO_4^{3-} sites) is present, because it is difficult to distinguish PO_4^{3-} from HPO_4^{2-}
731 using standard colorimetric techniques. Instead, carefully calibrated IR techniques must be used
732 (Eichert et al. 2009).

733 An essential distinction to recognize in Ca-P materials is the difference between
734 stoichiometric HA and "calcium-deficient apatite" (CDA). The long-used term CDA
735 unfortunately can create misunderstandings between the mineralogical and materials
736 communities, since all biological carbonated apatite is calcium deficient compared to HA, i.e.,
737 $\text{Ca}_{10-x}(\text{PO}_4)_{6-x}(\text{CO}_3)_x(\text{OH})_{2-x}$ cf. $\text{Ca}_{10}(\text{PO}_4)_6(\text{OH})_2$. The medical and, by extension, the materials
738 science communities apply the term CDA with reference to the molar ratio of Ca:P rather than to
739 how many moles of Ca are in the unit cell. Whereas the Ca:P atomic ratio is 1.67 for
740 stoichiometric HA, the medically defined CDA has a ratio of 1.4-1.6. The distinction between
741 the mineralogical and materials science views of Ca deficiency arises because of a difference in
742 the dominant ion recognized to substitute for PO_4 . In the bioapatite formula above, the dominant
743 substitution is recognized as CO_3^{2-} for PO_4^{3-} . According to the above formula, CO_3^{2-} substitution
744 causes a decrease in the [Ca] of the apatite, but an increase in the Ca:P ratio to values exceeding
745 1.67 as a function of $(10-x)/(6-x)$, where x = the number of moles of CO_3^{2-} . The medical and
746 biomaterials communities, however, often exclude CO_3 physically as well as conceptually in
747 their formulations. For them the pertinent substitution is often recognized as HPO_4^{2-} for PO_4^{3-} ,
748 i.e., $\text{Ca}_{10-x}(\text{PO}_4)_{6-x}(\text{HPO}_4)_x(\text{OH})_{2-x}$. The resultant Ca:P ratio is $(10-x)/6$ rather than $(10-x)/(6-x)$,
749 where x = the number of moles of HPO_4^{2-} . The difference in the effect on the Ca:P ratio of

750 apatite by CO_3^{2-} vs. HPO_4^{2-} substitution is that the substituent HPO_4^{2-} contains P. Increasing
751 substitution for PO_4^{3-} by HPO_4^{2-} therefore leads to a decrease in Ca:P, thus, formation of
752 calcium-deficient apatite, CDA. LeGeros et al. (2003) more broadly defined CDA as $\text{Ca}_{10-x}\text{M}_x(\text{PO}_4)_6-y(\text{HPO}_4)_y(\text{OH})_2$, where M is a Ca-substituting cation such as Mg^{2+} or Na^+ , the
753 incorporation of which would further decrease Ca concentration.
754

755 The materials-community-defined CDA shows lower degrees of crystallinity than does
756 HA, as documented by CDA's broader (as well as weaker) X-ray diffraction peaks (reflecting
757 smaller crystallite sizes) and broader Raman and IR peaks (reflecting greater atomic disorder).
758 The *a*-axis dimension of the unit cell of CDA is larger than that for HA (9.438-9.461 Å for CDA
759 compared to 9.422 Å for HA) likely due to substitution of $(\text{HPO}_4)^{2-}$ for $(\text{PO}_4)^{3-}$, as indicated by
760 an IR absorption peak at about 864 cm^{-1} (LeGeros et al. 2009). One of the most straightforward
761 ways to evaluate the Ca:P ratio of an apatite is to sinter it above $800\text{ }^\circ\text{C}$, which will yield only
762 HA if the sample's bulk Ca:P = 1.67, but a mixture of HA + CaO if Ca:P > 1.67 or HA + β -TCP
763 if Ca:P < 1.67 (LeGeros 1981; LeGeros et al. 2003).

764 X-ray powder diffraction is very useful for phase identification, e.g., of HA. However,
765 the broad peaks associated with nanocrystalline apatite, indicative of small crystallite size, make
766 it difficult to infer compositional attributes and to detect the presence of additional phases simply
767 by XRD (see Figure 5). In addition, octacalcium phosphate, $\text{Ca}_8\text{H}_2(\text{PO}_4)_6 \cdot 5\text{H}_2\text{O}$, OCP, has an
768 XRD pattern very similar to that of HA, and amorphous calcium phosphate produces only a
769 broad featureless hump at $27\text{-}40^\circ$ and a much weaker feature at $50\text{-}60^\circ\ 2\Theta$ using Cu-K_α radiation
770 (Eichert et al. 2009). In X-ray powder diffraction, one can assess the peak profile for line-
771 broadening indicative of crystallite size (via the Scherrer equation), as distinguished from

772 "microstrain" in the crystallites (Danilchenko et al. 2002). Baig et al. (1999) used Rietveld
773 analysis of XRD data to infer microstrain, which they believed exerted the major control on the
774 solubility of nanocrystalline apatite. In contrast, Eichert et al. (2009) concluded that the XRD
775 features attributed to microstrain actually might more strongly reflect compositional
776 heterogeneity within the sample. Our own research in applying Raman microprobe spectroscopy
777 to carbonated HA samples aqueously precipitated at 60-80 °C confirms such heterogeneity with
778 respect to carbonate concentration (Pasteris and Yoder, unpublished). TEM images of synthetic
779 apatite precipitates often indicate larger dimensions than XRD-derived size values for the same
780 samples (Alix Deymier, pers. comm.). This consistent mismatch appears to reflect the difference
781 between crystallites (length-scales of lattice continuity defined by XRD) and particles (TEM-
782 imaged objects, which in some cases may be aggregates of crystallites).

783 IR and Raman spectral band positions can be used to distinguish among the various Ca-P
784 phases (Wopenka and Pasteris 2005; Eichert et al. 2009), as well as to document the presence of
785 OH and H₂O (Fig. 5b) and, to some degree, to indicate chemical substitutions (e.g., F for OH).
786 IR is especially effective in distinguishing between A-type and B-type carbonate substitution for
787 OH or PO₄, respectively (Penel et al. 1998; Rey et al. 2007a; Wopenka and Pasteris 2005;
788 Eichert et al. 2009). Deconvolution of the observed IR peaks into recognized underlying bands
789 (see Figure 6) reveals the important distinction between the phosphate and carbonate groups that
790 are structurally incorporated in the lattice ("apatitic") and those groups adsorbed in the hydration
791 layer, i.e., "non-apatitic" (Rey et al. 2007a). Band widths in Raman and IR spectra (Fig. 5b)
792 reflect the degree of atomic order in the apatite, where narrower bands indicate a higher degree
793 of order (Penel et al. 1998; McElderry et al. 2013). With the application of a laboratory-specific

794 calibration curve, one can determine the weight% carbonate substituted in an apatite sample
795 based on the Raman spectrum (Awonusi et al. 2007; Li et al. 2013) or IR spectrum.

796 Several other analyses provide direct characterization information or data that can aid
797 prediction of the apatite's biological response. For instance, the wettability of the
798 nanocrystalline apatite (actually, of its surface) helps control cell adhesion (Lim and Donahue
799 2004). Hydration-layer-controlled surface reactivity helps define the setting reaction(s) in a Ca-
800 P cement and how strongly an apatite coating adheres to its substrate (Rey et al. 2007a).

801 Several papers are extremely useful references because they either examine the relation
802 between experimental synthesis methods (including post-synthesis treatment) and the physico-
803 chemical properties of the apatites produced (e.g., Koutsopoulos 2002), or they effectively
804 document how to apply multiple analytical techniques to a suite of synthesized Ca-P materials.
805 For example, Sprio et al. (2008) synthesized multi-substituted (Si, Mg, CO₃) apatites and
806 characterized them by XRD (phase analysis, crystallinity), FTIR (multiple spectral regions; B-
807 type vs. A-type CO₃ substitution, effect of CO₃ substitution on [OH], H₂O adsorption), ICP bulk
808 chemical analysis, BET (specific surface area, reflecting particle size), thermal analysis by TGA
809 and DTA (temperature of CO₂ release, wt% CO₃ in apatite; thermal stability), and solubility tests
810 (distinguishing effects of Si, Mg, and CO₃). Bang et al. (2014) also synthesized and analyzed
811 CO₃- and Si-CO₃-substituted hydroxylapatites. In addition to XRD (lattice parameters and
812 crystallite size), FTIR, solubility measurement, and ICP (for Si and Ca) analysis, Bang et al.
813 (2014) added XRF (for Ca:P analysis) and mechanical properties tests for tensile strength.
814 LeGeros and LeGeros (1993), Eichert et al. (2009), and Drouet (2013) summarized the
815 application of a number of techniques to synthetic nanocrystalline apatites, relating properties to

816 synthesis conditions in many cases. Rey et al. (2007a,b) summarized their earlier work in IR
817 spectroscopy to tease apart information on apatitic (i.e., crystallographically incorporated) vs.
818 non-apatitic (i.e., adsorbed) PO₄, HPO₄, CO₃, and H₂O in nanocrystalline biological and
819 synthetic apatite.

820 Various types of NMR spectroscopy have been applied to bone and synthetic apatite in
821 the past several decades (Jäger et al. 2006; Kolmas and Kolodziejewski 2007), typically to identify
822 the presence of specific ions involving the elements H, P, and C and their abundance, as in the
823 case of hydroxyl (Cho et al. 2003; Kolmas et al. 2012). NMR data also helped to clarify the
824 siting of molecular and ionic species in the apatite structure, for instance, that of molecular H₂O
825 (Wilson et al. 2006a), as summarized in Pasteris (2012). NMR has been used to distinguish
826 compositional components within the core of apatite crystals from those in the hydration shell
827 (Jäger et al. 2006; Drouet 2013). It also has been applied to interpret plasma-sprayed
828 hydroxylapatite coatings (Heimann 2012). Additional information on the fabricated forms and
829 fabrication processes of specific types of biomaterials (e.g., apatite cements, apatitic coatings,
830 and bioactive glass) can be found in the online supplement.

831

832 **Factors that Control the Success of Apatitic Biomaterials**

833 As described above, there are widely varying functions for which apatitic materials have
834 been formulated. In some cases, the apatite enables better functionality of another biomaterial
835 (e.g., a metal), whereas in other cases, the apatite IS the biomaterial (e.g., porous HA blocks).
836 Some of the characteristics of greatest significance to apatitic biomaterials are their surface
837 properties (smooth, rough, with or without asperities), particle size, specific composition (e.g.,

838 Ca:P ratio and concentration of Mg and CO₃), porosity (pore size and percent of bulk material),
839 ability to incorporate and be biocompatible with cells and bioactive molecules, mechanical
840 properties (e.g., hardness, stiffness, wear resistance), and solubility in body fluid (Kretlow and
841 Mikos 2007). Even if osteogenic responses can be measured, however, the mechanisms behind
842 them are not always clear. For instance, less crystalline or amorphous apatite is more readily
843 resorbable, but better crystalline (especially carbonated) apatite encourages more cell adsorption
844 and proliferation (Surmenev et al. 2014; Nakamura et al. 2016).

845 Drouet et al. (2009) summarized very clearly the results of their many types of
846 experiments in low-temperature aqueous precipitation of apatite, as well as their chosen mineral
847 characterization techniques. They described how changes to the temperature and pH of the
848 synthesis solution, as well as the maturation time during which the precipitates remained in the
849 solution, can be used to tailor such characteristics of apatite nanoparticles as the crystallite size,
850 bioresorbability, degree of crystallinity, degree of non-stoichiometry, physical extent of
851 hydration layer, ion concentration in non-apatitic sites (i.e., in the hydration layer rather than in
852 the crystal lattice), and the bulk chemical composition (including Ca:P, [HPO₄²⁻]).

853 LeGeros et al. (2003) described the history of the development of biphasic calcium
854 phosphate, BCP (i.e., HA + β-TCP), including how the HA:TCP ratio is controlled. BCP
855 formation begins with precipitation of a Ca-deficient HA, which is then sintered at 700 °C. The
856 more Ca-deficient the original material, the greater the proportion of TCP after sintering.
857 Additional substituting ions in the precursor material also affect the HA:TCP ratio. For instance,
858 structural incorporation of CO₃²⁻ and Mg²⁺ in the unsintered material causes an increase in the
859 HA:TCP of the sintered product. If the initial aqueous synthesis step is done at “high”

860 temperature (80 - 100 °C) but low pH (4-6), a CDA phase of relatively high crystallinity and
861 large crystal size develops, in contrast to the much less crystalline CDA formed at the same
862 temperature but at a pH of 9 (LeGeros et al. 2003).

863 Pore size in bone cement can be controlled by the grain size of the reactant compounds
864 and the relative solubility of the compounds (as in Ca-S + HA mixtures). The pore dimensions
865 control both the bioactivity of the material (vascularization, cell incorporation) and its drug-
866 delivery capability. The degree of crystallinity (a function of thermal processing and ion
867 substitution) strongly affects solubility and therefore resorption rate of the cement, as does the
868 crystallite size (Ginebra et al. 2012).

869 The materials science community has recently begun to explore the effects of carbonate
870 concentration in synthetic apatite on the body's cellular response. Adams et al. (2014) reported
871 that elevation of carbonate concentration in apatite increased the number of osteoblast-like (i.e.,
872 bone-forming) cells attracted to the surface of synthetic apatite discs. However, such increases
873 in carbonate also decreased the degree of differentiation of the osteoblasts, suggesting that they
874 would be less able and likely to induce mineralization. In analogous types of experiments,
875 Nakamura et al. (2016) determined more recently that higher carbonate concentration in
876 synthetic apatite favored the differentiation of bone marrow cells into osteoclasts (bone-
877 resorbing cells), thereby inducing more resorption of bone. Such experiments indicate that the
878 carbonate concentration in apatitic biomaterials could be tailored for specific purposes, such as
879 temporary scaffolding that subsequently would be removed/resorbed within a controlled time-
880 frame (Adams et al. 2014; Nakamura et al. 2016).

881

882

Implications

883

Research into the development of biomaterials offers mineralogists and geochemists a

884

novel view of the adaptability of the apatite structure and its implications for human health.

885

Biomaterials research highlights (1) the important effects of synthesis techniques on the

886

properties developed in a chemically and structurally accommodating phase such as apatite, (2)

887

the applicability of cutting-edge analytical techniques in the characterization of mineral

888

properties, especially those of nanocrystalline phases, (3) the importance of a mineral's surface

889

chemistry, including the presence of water and adsorbed ions, and (4) how this calcium-

890

phosphate mineral remains "apatite" throughout such a wide range of compositional substitutions

891

and consequent structural perturbations. The key to the latter is a kind of chemical-structural

892

choreography that assures the nature of the ions and their spatial positioning remain

893

appropriately synchronized. The formulation, synthesis procedures, and analytical

894

characterization of apatitic biomaterials before, during, and after implantation in a living creature

895

(typically a human) provide unique non-geological examples of the power of mineralogy.

896

Biomaterials research clearly is not one of the new subfields, such as geobiology or

897

biomineralization, that have become important in the geosciences. However, we geoscientists

898

should consider viewing biomaterials as a major subfield of materials research that offers

899

opportunities for both observation and participation by the broader mineralogical-geochemical

900

community.

901

902

Acknowledgments

903

Development of the paper was supported in part by NIH grant 5U01EB01642202.

904 Discussions over many years with Claude Yoder concerning apatite synthesis were very helpful
905 to the writing of this review. Thoughtful comments on an earlier version of the manuscript by
906 three reviewers, Robert Heimann, Catherine Skinner, and an anonymous reviewer are much
907 appreciated. The author, however, should be held responsible for all statements and opinions in
908 the article.

909

910

Reference List

911

912 Adams, B.R., Mostafa, A., Schwartz, Z., and Boyan, B.D. (2014) Osteoblast response to
913 nanocrystalline calcium hydroxyapatite depends on carbonate content. *Journal of Biomedical*
914 *Materials Research Part A*, 102A, 3237-3242.

915 Afzal, A. (2014) Implantable zirconia bioceramics for bone repair and replacement: A
916 chronological review. *Materials Express*, 4, 1-12.

917 Albright, J.A. and Skinner, H.C.W. (1987) Bone: Structural organization and remodeling
918 dynamics. In J.A. Albright and R.A. Brand, Eds. *The Scientific Basis of Orthopaedics*, p. 161-
919 198, Appleton and Lange, Norwalk, CT.

920 Albee, F.H. and Morrison, H.F. (1920) Studies in bone growth: Triple calcium phosphate as a
921 stimulus to osteogenesis. *Annals of Surgery*, 71, 32-39.

922 Alexander, B., Daulton, T.L., Genin, G.M., Lipner, J., Pasteris, J.D., Wopenka, B., and
923 Thomopoulos, S. (2012) The nanometre-scale physiology of bone: Steric modelling and
924 scanning transmission electron microscopy of collagen-mineral structure. *Journal of the Royal*
925 *Society Interface*, 9, 1774-1786.

926 Awonusi, A., Morris, M.D., and Tecklenburg, M.M.J. (2007) Carbonate assignment and
927 calibration in the Raman spectrum of apatite. *Calcified Tissue International*, 81, 46-52.

928 Baig, A.A., Fox, J.L., Young, R.A., Wang, Z., Hsu, J., Higuchi, W.I., Chhetry, A., Zhuang, H.,
929 and Otsuka, M. (1999) Relationships among carbonated apatite solubility, crystallite size, and
930 microstrain parameters. *Calcified Tissue International*, 64, 437-449.

931 Bakan, F., Lacin, O., and Sarac, H. (2013) A novel low temperature sol-gel synthesis process for
932 thermally stable nano crystalline hydroxyapatite. *Powder Technology*, 233, 295-302.

933 Bang, L.T., Long, B.D., and Othman, R. (2014) Carbonate hydroxyapatite and silicon-substituted
934 carbonate hydroxyapatite: Synthesis, mechanical properties, and solubility evaluations. *The*

- 935 Scientific World Journal, 2014, article ID 969876.
- 936 Basu, B. and Nath, S. (2009) Fundamentals of biomaterials and biocompatibility. In B. Basu, D.
937 Katti, and A. Kumar, Eds., *Advanced Biomaterials: Fundamentals, Processing, and Applications*,
938 p. 3-18, John Wiley & Sons, Inc., Hoboken, NJ.
- 939 Bayazit, V., Bayazit, M., and Bayazit, E. (2010) Evaluation of bioceramic materials in biology
940 and medicine. *Digest Journal of Nanomaterials and Biostructures*, 7, 211-222.
- 941 Beevers, C.A. and McIntyre, D.B. (1946) The atomic structure of fluor-apatite and its relation to
942 that of tooth and bone material. *Mineralogical Magazine*, 27, 254-257.
- 943 Bertinetti, L., Drouet, C., Combes, C., Rey, C., Tampieri, A., Coluccia, S., and Martra, G. (2009)
944 Surface characteristics of nanocrystalline apatites: Effect of Mg surface enrichment on
945 morphology, surface hydration species, and cationic environments. *Langmuir*, 25, 5647-5654.
- 946 Biltz, R.M. and Pellegrino, E.D. (1969) The chemical anatomy of bone: I. A comparative study
947 of bone composition in sixteen vertebrates. *Journal of Bone and Joint Surgery*, 51, 456-466.
- 948 Boivin, G. (2007) The hydroxyapatite crystal: A closer look. *Medicographia*, 29, 126-132.
- 949 Bonfield, W., Grynopas, M.D., Tully, A.E., Bowman, J., and Abram, J. (1981) Hydroxyapatite
950 reinforced polyethylene -- A mechanically compatible implant material for bone replacement.
951 *Biomaterials*, 2, 185-186.
- 952 Borkiewicz, O., Rakovan, J., and Cahill, C.L. (2010) Time-resolved in situ studies of apatite
953 formation in aqueous solutions. *American Mineralogist*, 95, 1224-1236.
- 954 Boskey, A. (2007) Mineralization of bones and teeth. *Elements*, 3, 385-391.
- 955 Boudeville, P., Pauvert, B., Ginebra, M.P., Fernandez, E., and Planell, J.A. (2001) Dry
956 mechanosynthesis of apatites and other calcium phosphates. *Key Engineering Materials*, 192-
957 195, 115-118.
- 958 Brown, P.W. (1992) Phase relationships in the ternary system CaO-P₂O₅-H₂O at 25 °C. *Journal*
959 *of the American Ceramic Society*, 75, 17-22.
- 960 Brown, P.W., Hocker, N., and Hoyle, S. (1991) Variations in solution chemistry during the low-
961 temperature formation of hydroxyapatite. *Journal of the American Ceramic Society*, 74, 1848-
962 1854.
- 963 Bushinsky, D.A., Smith, S.B., Gavrilov, K.L., Gavrilov, L.F., Li, J., and Levi-Setti, R. (2002)
964 Acute acidosis-induced alteration in bone bicarbonate and phosphate. *American Journal of*
965 *Physiology - Renal Physiology*, 283, F1091-F1097.

- 966 Carayon, M.T. and Lacout, J.L. (2003) Study of the Ca/P atomic ratio of the amorphous phase in
967 plasma-sprayed hydroxyapatite coatings. *Journal of Solid State Chemistry*, 172, 339-350.
- 968 Carlson, S.J. (1990) Vertebrate dental structures. In J.G. Carter, Ed., *Skeletal Biomineralization:
969 Patterns, Processes and Evolutionary Trends*, vol. 1, p. 531-556, Van Nostrand Rheinhold, New
970 York.
- 971 Chaikina, M.V., Khlusov, I.A., Karlov, A.V., and Paichadze, K.S. (2004) Mechanochemical
972 synthesis of nonstoichiometric and substituted apatites with nanosized particles for use as
973 biologically compatible materials. *Chemistry for Sustainable Development*, 12, 385-394.
- 974 Chaudhry, A.A., Knowles, J.C., Rehman, I., and Darr, J.A. (2012) Rapid hydrothermal flow
975 synthesis and characterisation of carbonate- and silicate-substituted calcium phosphates. *Journal
976 of Biomaterials Applications*, 28, 448-461.
- 977 Chen, P.-Y., Stokes, A.G., and McKittrick, J. (2009) Comparison of the structure and mechanical
978 properties of bovine femur bone and antler of the North American elk. *Acta Biomaterialia*, 5,
979 693-706.
- 980 Chen, P.-Y., Toroian, D., Price, P.A., and McKittrick, J. (2011) Minerals form a continuum
981 phase in mature cancellous bone. *Calcified Tissue International*, 88, 351-361.
- 982 Cho, G., Wu, Y., and Ackerman, J.L. (2003) Detection of hydroxyl ions in bone mineral by
983 solid-state NMR spectroscopy. *Science*, 300, 1123-1127.
- 984 Cho, J.S., Um, S.-H., Yoo, D.S., Chung, Y.-C., Chung, S.H., Lee, J.-C., and Rhee, S.-H. (2013)
985 Enhanced osteoconductivity of sodium-substituted hydroxyapatite by system instability. *Journal
986 of Biomedical Materials Research Part B*, 102B, 1046-1062.
- 987 Currey, J.D. (2006) *Bones: Structure and Mechanics*, Princeton University Press, Princeton.
- 988 Currey, J.D., Landete-Castillejos, T., Estevez, J., Ceacero, F., Olguin, A., Garcia, A., and
989 Gallego, L. (2009) The mechanical properties of red deer antler bone when used in fighting. *The
990 Journal of Experimental Biology*, 212, 3985-3993.
- 991 Daculsi, G., Bouler, J.J., and LeGeros, R.Z. (1997) Adaptive crystal formation in normal and
992 pathological calcifications in synthetic calcium phosphate and related biomaterials. *International
993 Review of Cytology*, 172, 129-189.
- 994 Daculsi, G., Jegoux, F., and Layrolle, P. (2009) The micro macroporous biphasic calcium
995 phosphate concept for bone reconstruction and tissue engineering. In B. Basu, D. Katti, and A.
996 Kumar, Eds., *Advanced Biomaterials: Fundamentals, Processing, and Applications*, p. 101-141,
997 John Wiley & Sons, New York.
- 998 Daculsi, G., LeGeros, R.Z., Durand, M., Borget, P., Baroth, S., Goyenville, E., Aguado, E., and

- 999 Jegoux, F. (2010) Injectable apatitic calcium phosphate cements and microporous biphasic
1000 calcium phosphate granules. *Journal of the Australian Ceramic Society*, 46, 1-5.
- 1001 Danilchenko, S.N., Kukharenko, O.G., Moseke, C., Protsenko, I.Y., Sukhodub, L.F., and Sulki-
1002 Cleff, B. (2002) Determination of the bone mineral crystallite size and lattice strain from line
1003 broadening. *Crystal Research and Technology*, 37, 1234-1240.
- 1004 Deshpande, A.S. and Beniash, E. (2008) Bioinspired synthesis of mineralized collagen fibrils.
1005 *Crystal Growth and Design*, 8, 3084-3090.
- 1006 Dorozhkin, S.V. (2010) Bioceramics of calcium phosphate. *Biomaterials*, 31, 1465-1485.
- 1007 Dorozhkin, S.V. (2012a) Amorphous calcium orthophosphates: Nature, chemistry and
1008 biomedical applications. *International Journal of Materials and Chemistry*, 2, 19-46.
- 1009 Dorozhkin, S.V. (2012b) Calcium orthophosphate coatings, films, and layers. *Progress in*
1010 *Biomaterials*, 1, 1-40.
- 1011 Driessens, F.C.M. and Verbeeck, R.M.H. (1990) *Biominerals*, CRC Press, Boca Raton.
- 1012 Drouet, C. (2013) Apatite formation: Why it may not work as planned, and how to conclusively
1013 identify apatite compounds. *BioMed Research International*, 2013, ID 490946, 12 pp.
- 1014 Drouet, C., Bosc, F., Banu, M., Largeot, C., Combes, C., Dechambre, G., Estournes, C.,
1015 Raimbeaux, G., and Rey, C. (2009) Nanocrystalline apatites: From powders to biomaterials.
1016 *Powder Technology*, 190, 118-122.
- 1017 Eichert, D., Drouet, C., Sfihi, H., Rey, C., and Combes, C. (2009) *Nanocrystalline Apatite-Based*
1018 *Biomaterials*, Nova Science Publishers, Inc., New York.
- 1019 Ellies, L.G., Carter, J.M., Natiella, J.R., Featherstone, J.D.B., and Nelson, D.G.A. (1988)
1020 Quantitative analysis of early in vivo tissue response to synthetic apatite implants. *Journal of*
1021 *Biomedical Materials Research*, 22, 137-148.
- 1022 Elliott, J.C. (1994) *Structure and Chemistry of the Apatites and Other Calcium Orthophosphates*,
1023 Elsevier, New York.
- 1024 Elliott, J.C. (2002) Calcium phosphate biominerals. In M.J. Kohn, J. Rakovan, and J.M. Hughes,
1025 Eds., *Phosphates – Geochemical, Geobiological, and Materials Importance*, 48, p. 427-453.
1026 *Reviews in Mineralogy and Geochemistry*, Mineralogical Society of America, Chantilly,
1027 Virginia.
- 1028 Elmore, K.L. and Farr, T.D. (1940) Equilibrium in the system calcium oxide-phosphorus
1029 pentoxide-water. *Industrial and Engineering Chemistry*, 32, 580-586.

- 1030 Ewing, R.C. and Wang, L. (2002) Phosphates as nuclear waste forms. In M.J. Kohn, J. Rakovan,
1031 and J.M. Hughes, Eds., Phosphates – Geochemical, Geobiological, and Materials Importance, p.
1032 673-700. Reviews in Mineralogy and Geochemistry, Mineralogical Society of America,
1033 Chantilly, VA.
- 1034 Fahami, A., Nasiri-Tabrizi, B., Beall, G.W., and Pinguan-Murphy, B. (2015) Effect of ion
1035 concentration on mechanosynthesis of carbonated chlorapatite nanopowders. Materials Letters,
1036 146, 16-19.
- 1037 Feng, S.-S. and Rockett, T.J. (1979) The system CaO-P₂O₅-H₂O at 200 °C. Journal of the
1038 American Ceramic Society, 62, 619-620.
- 1039 Ferrario, V.F., Sforza, C., Serrao, G., Dellavia, C., and Tartaglia, G.M. (2004) Single tooth bite
1040 force in healthy young adults. Journal of Oral Rehabilitation, 31, 18-22.
- 1041 Fleet, M. (2015) Carbonated Hydroxyapatite: Materials, Synthesis, and Applications, Pan
1042 Stanford Publishing, Singapore.
- 1043 Fox, M. and Shuster, D.L. (2014) The influence of burial heating on the (U-Th)/He system in
1044 apatite: Grand Canyon case study. Earth and Planetary Science Letters, 397, 174-183.
- 1045 Ginebra, M.-P., Canal, C., Espanol, M., Pastorino, D., and Montufar, E.B. (2012) Calcium
1046 phosphate cements as drug delivery materials. Advanced Drug Delivery Reviews, 64, 1090-
1047 1110.
- 1048 Glimcher, M.J. (2006) Bone: Nature of the calcium phosphate crystals and cellular, structural,
1049 and physical chemical mechanisms in their formation. In N. Sahai and M.A.A. Schoonen, Eds.,
1050 Medical Mineralogy and Geochemistry, 64, p. 223-282. Reviews in Mineralogy and
1051 Geochemistry, Mineralogical Society of America, Chantilly, Virginia.
- 1052 Goldenberg, J.E., Wilt, Z.T., Schermerhorn, D.V., Pasteris, J.D., and Yoder, C.H. (2015)
1053 Structural effects on incorporated water in carbonated apatites. American Mineralogist, 100, 274-
1054 280.
- 1055 Gross, K.A. and Berndt, C.C. (2002) Biomedical application of apatites. In M.J. Kohn, J.
1056 Rakovan, and J.M. Hughes, Eds., Phosphates – Geochemical, Geobiological and Material
1057 Importance, 48, p. 631-672. Reviews in Mineralogy and Geochemistry, Mineralogical Society of
1058 America, Chantilly, Virginia.
- 1059 Grynopas, M. (2007) Transient precursor strategy or very small biological apatite crystals? Bone,
1060 41, 162-164.
- 1061 Habraken, W., Habibovic, P., Epple, M., and Bohner, M. (2016) Calcium phosphates in
1062 biomedical applications: Materials for the future? Materials Today, 19, 69-87.

- 1063 Harrison, T.M., Catlos, E.J., and Montel, J.-M. (2002) U-Th-Pb dating of phosphate minerals. In
1064 M.J. Kohn, J. Rakovan, and J.M. Hughes, Eds., Phosphates -- Geochemical, Geobiological, and
1065 Materials Importance, 48, p. 523-558. Reviews in Mineralogy and Geochemistry, Mineralogical
1066 Society of America, Chantilly, Virginia.
- 1067 He, G., Dahl, T., Veis, A., and George, A. (2003) Nucleation of apatite crystals *in vitro* by self-
1068 assembled dentin matrix protein 1. *Nature Materials*, 2, 552-558.
- 1069 Heimann, R.B. (2012) Laser-Raman, nuclear magnetic resonance (NMR) and electron energy
1070 loss (EEL) spectroscopy studies of plasma-sprayed hydroxyapatite coatings. In R.B. Heimann,
1071 Ed., Calcium Phosphate: Structure, Synthesis, Properties, and Applications, p. 215-230, Nova
1072 Science Publishers, Inc., New York.
- 1073 Heimann, R.B. (2013) Structure, properties, and biomedical performance of osteoconductive
1074 bioceramic coatings. *Surface & Coatings Technology*, 233, 27-38.
- 1075 Heimann, R.B. (2016) Plasma-sprayed hydroxylapatite-based coatings: Chemical, mechanical,
1076 microstructural, and biomedical properties. *Journal of Thermal Spray Technology*, 25, in press.
- 1077 Heimann, R.B. and Lehmann, H.D. (2015) *Bioceramic Coatings for Medical Implants*, Wiley-
1078 VCH, Berlin.
- 1079 Heimann, R.B., Vu, T.A., and Wayman, M.L. (1997) Bioceramic coatings: State-of-the-art and
1080 recent development trends. *European Journal of Mineralogy*, 9, 597-615.
- 1081 Hench, L.L. (1998) Bioceramics. *Journal of the American Ceramic Society*, 81, 1705-1728.
- 1082 Hench, L.L. and Wilson, J. (1993) *An Introduction to Bioceramics*, World Scientific, Singapore.
- 1083 Hing, K.A., Wilson, L.F., and Buckland, T. (2007) Comparative performance of three ceramic
1084 bone graft substitutes. *The Spine Journal*, 7, 475-490.
- 1085 Hongmin, L., Wei, Z., Xingrong, Y., Jing, W., Wenxin, G., Jihong, C., Xin, X., and Fulin, C.
1086 (2015) Osteoinductive nanohydroxyapatite bone substitute prepared via in situ hydrothermal
1087 transformation of cuttlefish bone. *Journal of Biomedical Materials Research, Part B*, 103B, 816-
1088 824.
- 1089 Hughes, J.M. (2015) The many facets of apatite. *American Mineralogist*, 100, 1033-1039.
- 1090 Hughes, J.M., Cameron, M., and Crowley, K.D. (1989) Structural variations in natural F, OH,
1091 and Cl apatites. *American Mineralogist*, 74, 870-876.
- 1092 Ihlen, P.M., Schiellerup, H., Gautneb, H., and Skar, O. (2014) Characterization of apatite
1093 resources in Norway and their REE potential – A review. *Ore Geology Reviews*, 58, 126-147.

- 1094 Jäger, C., Welzel, T., Meyer-Zaika, W., and Epple, M. (2006) A solid-state NMR investigation
1095 of the structure of nanocrystalline hydroxyapatite. *Magnetic Resonance in Chemistry*, 44, 573-
1096 580.
- 1097 Johnsson, M.S.A. and Nancollas, G.H. (1992) The role of brushite and octacalcium phosphate in
1098 apatite formation. *Critical Reviews in Oral Biology and Medicine*, 3, 61-82.
- 1099 Jones, J.R. (2013) Review of bioactive glass: From Hench to hybrids. *Acta Biomaterialia*, 9,
1100 44547-4486.
- 1101 Jugdaohsingh, R. (2007) Silicon and bone health. *Journal of Nutrition Health and Aging*, 11, 99-
1102 110.
- 1103 Kanayama, K., Sriarj, W., Shimokawa, H., Ohya, K., Doi, Y., and Shibutani, T. (2011)
1104 Osteoclast and osteoblast activities on carbonate apatite plates in cell cultures. *Journal of*
1105 *Biomaterials Applications*, 26, 435-449.
- 1106 Kim, I.-S. and Kumta, P.N. (2004) Sol-gel synthesis and characterization of nanostructured
1107 hydroxyapatite powder. *Materials Science and Engineering B*, 111, 232-236.
- 1108 Knudsen, A.C. and Gunter, M.E. (2002) Sedimentary phosphates – An example: Phosphoria
1109 Formation. In M.J. Kohn, J. Rakovan, and J.M. Hughes, Eds., *Phosphates – Geochemical,*
1110 *Geobiological, and Materials Importance*, 48, p. 363-389. *Reviews in Mineralogy and*
1111 *Geochemistry*, Mineralogical Society of America, Chantilly, Virginia.
- 1112 Kohn, M.J., Rakovan, J., and Hughes, J.M. (2002) *Phosphates – Geochemical, Geobiological,*
1113 *and Materials Importance*, Mineralogical Society of America, Chantilly, VA.
- 1114 Kohyama, K., Hatakeyama, E., Sasaki, T., Dan, H., Azuma, T., and Keishiro, K. (2004) Effects
1115 of sample hardness on human chewing force: A model study using silicone rubber. *Archives of*
1116 *Oral Biology*, 49, 805-816.
- 1117 Kolmas, J. and Kolodziejcki, W. (2007) Concentration of hydroxyl groups in dental apatites: A
1118 solid-state ^1H MAS NMR study using inverse ^{31}P -- ^1H cross-polarization. *Chemical*
1119 *Communications*, 2007, 4390-4392.
- 1120 Kolmas, J., Szwaja, M., and Kolodziejcki, W. (2012) Solid-state NMR and IR characterization of
1121 commercial xenographic biomaterials used as bone substitutes. *Journal of Pharmaceutical and*
1122 *Biomedical Analysis*, 61, 136-141.
- 1123 Koutsopoulos, S. (2002) Synthesis and characterization of hydroxyapatite crystals: A review
1124 study on the analytical methods. *Journal of Biomedical Materials Research*, 62, 600-612.
- 1125 Kreidler, E.R. and Hummel, F.A. (1967) Phase relationships in the system $\text{SrO-P}_2\text{O}_5$ and the
1126 influence of water vapor on the formation of $\text{Sr}_4\text{P}_2\text{O}_9$. *Inorganic Chemistry*, 6, 884-891.

- 1127 Kretlow, J.D. and Mikos, A.G. (2007) Review: Mineralization of synthetic polymer scaffolds for
1128 bone tissue engineering. *Tissue Engineering*, 13, 927-938.
- 1129 Kuriakose, T.A., Kalkura, S.N., Palanichamy, M., Arivuoli, D., Dierks, K., Bocelli, G., and
1130 Betzel, C. (2004) Synthesis of stoichiometric nano crystalline hydroxyapatite by ethanol-based
1131 sol-gel technique at low temperature. *Journal of Crystal Growth*, 263, 517-523.
- 1132 Landis, W.J. and Jacquet, R. (2013) Association of calcium and phosphate ions with collagen in
1133 the mineralization of vertebrate tissues. *Calcified Tissue International*, 93, 329-337.
- 1134 Lee, E.J., Kasper, F.K., and Mikos, A.G. (2014) Biomaterials for tissue engineering. *Annals of*
1135 *Biomedical Engineering*, 42, 323-337.
- 1136 LeGeros, R.Z. (1981) Apatites in biological systems. *Progress in Crystal Growth and*
1137 *Characterization of Materials*, 4, 1-45.
- 1138 LeGeros, R.Z. (1988) Calcium phosphate materials in restorative dentistry: A review. *Advances*
1139 *in Dental Research*, 2, 164-180.
- 1140 LeGeros, R.Z. (2008) Calcium phosphate-based osteoinductive materials. *Chemical Reviews*,
1141 108, 4742-4753.
- 1142 LeGeros, R.Z. and LeGeros, J.P. (1984) Phosphate minerals in human tissue. In J.O. Nriagu and
1143 P.B. Moore, Eds., *Phosphate Minerals*, p. 351-395, Springer-Verlag, New York.
- 1144 LeGeros, R.Z. and LeGeros, J.P. (1993) Dense hydroxyapatite. In L.L. Hench and J. Wilson,
1145 Eds., *An Introduction to Bioceramics*, p. 139-180. *Advanced Series in Ceramics*, vol. 1, World
1146 Scientific, Singapore.
- 1147 LeGeros, R.Z., Trautz, O.R., Klein, E., and LeGeros, J.P. (1969) Two types of carbonate
1148 substitution in the apatite structure. *Experientia*, 25, 5-7.
- 1149 LeGeros, R.Z., Bonel, G., and Legros, R. (1978) Types of "H₂O" in human enamel and in
1150 precipitated apatites. *Calcified Tissue International*, 26, 111-118.
- 1151 LeGeros, R.Z., Lin, S., Rohanizadeh, R., Mijares, D., and LeGeros, J.P. (2003) Biphasic calcium
1152 phosphate bioceramics: Preparation, properties and applications. *Journal of Materials Science:*
1153 *Materials in Medicine*, 14, 201-209.
- 1154 LeGeros, R.Z., Ito, A., Ishikawa, K., Sakae, T., and LeGeros, J.P. (2009) Fundamentals of
1155 hydroxyapatite and related calcium phosphates. In B. Basu, D. Katti, and A. Kumar, Eds.,
1156 *Advanced Biomaterials: Fundamentals, Processing, and Applications*, p. 19-52, John Wiley &
1157 Sons, Inc., Hoboken, NJ.
- 1158 Li, Z. and Pasteris, J.D. (2014) Chemistry of bone mineral, based on the hypermineralized

- 1159 rostrum of the beaked whale *Mesoplodon densirostris*. American Mineralogist, 99, 645-653.
- 1160 Li, Z., Pasteris, J.D., and Novack, D. (2013) Hypermineralized whale rostrum as the exemplar
1161 for bone mineral. Connective Tissue Research, 54, 167-175.
- 1162 Lim, J.Y. and Donahue, H.J. (2004) Biomaterial characteristics important to skeletal tissue
1163 engineering. Journal of Musculoskeletal and Neuronal Interactions, 4, 396-398.
- 1164 Liu, W.Y., Lipner, J., Xie, J.W., Manning, C.N., Thomopoulos, S., and Xia, Y.N. (2014)
1165 Nanofiber scaffolds with gradients in mineral content for spatial control of osteogenesis. ACS
1166 Applied Materials and Interfaces, 6, 2849-2856.
- 1167 Liu, X., Rahaman, M.N., Hilmas, G.E., and Bal, B.S. (2013) Mechanical properties of bioactive
1168 glass (13-93) scaffolds fabricated by robotic deposition for structural bone repair. Acta
1169 Biomaterialia, 9, 7025-7034.
- 1170 Liu, Y., Kim, Y.K., Dai, L., Li, N., Khan, S.O., Pashley, D.H., and Tay, F.R. (2011) Hierarchical
1171 and non-hierarchical mineralisation of collagen. Biomaterials, 32, 1291-1300.
- 1172 Luz, G.M. and Mano, J.F. (2011) Preparation and characterization of bioactive glass
1173 nanoparticles prepared by sol-gel for biomedical applications. Nanotechnology, 22, doi:
1174 10.1088/0957-4484/22/49/494014, 11 pp.
- 1175 McConnell, D. (1937) The substitution of SiO_4^- and SO_4^- groups for PO_4^- groups in the apatite
1176 structure; ellestadite, the end-member. American Mineralogist, 22, 977-986.
- 1177 McConnell, D. (1962) Same as: The crystal structure of bone. Clinical Orthopaedics, 23, 253.
- 1178 McElderry, J.-D.P., Zhu, P., Mroue, K.H., Xu, J., Pavan, B., Fang, M., Zhao, G., McNerny, E.,
1179 Kohn, D.H., Franceschi, R.T., and others (2013) Crystallinity and compositional changes in
1180 carbonated apatites: Evidence from ^{31}P solid-state NMR, Raman, and AFM analysis. Journal of
1181 Solid State Chemistry, 206, 192-198.
- 1182 Menanteau, J., Neuman, W.F., and Neuman, M.W. (1982) A study of bone proteins which can
1183 prevent hydroxyapatite formation. Metabolic Bone Disease & Related Research, 4, 157-162.
- 1184 Mochales, C., Wilson, R.M., Dowker, S.E.P., and Ginebra, M.-P. (2011) Dry mechanosynthesis
1185 of nanocrystalline calcium deficient hydroxyapatite: Structural characterisation. Journal of
1186 Alloys and Compounds, 509, 7389-7394.
- 1187 Mostafa, N.Y., Hassan, H.M., and Abd Ekaldar, O.H. (2011) Preparation and characterization of
1188 Na^+ , SiO_4^{4-} , and CO_3^{2-} co-substituted hydroxyapatite. Journal of the American Ceramic Society,
1189 94, 1584-1590.
- 1190 Nakamura, M., Hiratai, R., Hentunen, T., Salonen, J., and Yamashita, K. (2016) Hydroxyapatite

- 1191 with high carbonated substitutions promotes osteoclast resorption through osteocyte-like cells.
1192 ACS Biomaterials Science and Engineering, 2, 259-267.
- 1193 Naqshbandi, A.R., Sopyan, I., and Gunawan (2013) Development of porous calcium phosphate
1194 bioceramics for bone implant applications: A review. Recent Patents on Materials Science, 6,
1195 238-252.
- 1196 Nath, S. and Basu, B. (2009) Materials for orthopedic applications. In B. Basu, D. Katti, and A.
1197 Kumar, Eds., Advanced Biomaterials: Fundamentals, Processing, and Applications, p. 53-100,
1198 John Wiley & Sons, Inc., Hoboken, NJ.
- 1199 Neuman, W.F. and Neuman, M.W. (1953) The nature of the mineral phase of bone. Chemical
1200 Reviews, 53, 1-45.
- 1201 Neuman, W.F. and Neuman, M.W. (1958) The Chemical Dynamics of Bone Mineral, University
1202 of Chicago Press, Chicago.
- 1203 Nilsson, M., Zheng, M.H., and Tagil, M. (2013) The composite of hydroxyapatite and calcium
1204 sulphate: A review of preclinical evaluation and clinical applications. Expert Reviews of Medical
1205 Devices, 10, 675-684.
- 1206 Nudelman, F., Lausch, A.J., Sommerdijk, N.A.J.M., and Sone, E.D. (2013) In vitro models of
1207 collagen biomineralization. Journal of Structural Biology, 183, 258-269.
- 1208 Nudelman, F., Pieterse, K., George, A., Bomans, P.H., Friedrich, H., Brylka, L.J., Hilbers,
1209 P.A.J., de With, G., and Sommerdijk, N.A.J.M. (2010) The role of collagen in bone apatite
1210 formation in the presence of hydroxyapatite nucleation inhibitors. Nature Materials, 9, 1004-
1211 1009.
- 1212 Oliveira, A.L. and Reis, R.L. (2005) Bonelike apatite coatings nucleated on biodegradable
1213 polymers as a way to induce bone mineralization: Current developments and future trends. In
1214 R.L. Reis and J.S. Roman, Eds., Biodegradable Systems in Tissue Engineering and Regenerative
1215 Medicine, p. 205-217, CRC Press, Boca Raton, FL.
- 1216 Olszta, M.J., Cheng, X., Jee, S.S., Kumar, R., Kim, Y.-Y., Kaufman, M.J., Douglas, E.P., and
1217 Gower, L.B. (2007) Bone structure and formation: A new perspective. Materials Science and
1218 Engineering C, R58, 77-116.
- 1219 Pan, Y. and Fleet, M.E. (2002) Compositions of the apatite-group minerals: Substitution
1220 mechanisms and controlling factors. In M.J. Kohn, J. Rakovan, and J.M. Hughes, Eds.,
1221 Phosphates – Geochemical, Geobiological, and Materials Importance, 48, p. 13-49. Reviews in
1222 Mineralogy and Geochemistry, Mineralogical Society of America, Chantilly, Virginia.
- 1223 Pasteris, J.D. (2012) Structurally incorporated water in bone apatite: A cautionary tale. In R.B.
1224 Heimann, Ed., Calcium Phosphates: Structure, Synthesis, Properties, and Applications, p. 63-94,

- 1225 Nova Science Publishers, Inc., New York.
- 1226 Pasteris, J.D., Wopenka, B., and Valsami-Jones, E. (2008) Bone and tooth mineralization: Why
1227 apatite? *Elements*, 4, 97-104.
- 1228 Pasteris, J.D., Yoder, C.H., and Wopenka, B. (2014) Molecular water in nominally anhydrous
1229 carbonated hydroxylapatite: The key to a better understanding of bone mineral. *American*
1230 *Mineralogist*, 99, 16-27.
- 1231 Penel, G., Leroy, G., Rey, C., and Bres, E. (1998) MicroRaman spectral study of the PO₄ and
1232 CO₃ vibrational modes in synthetic and biological apatites. *Calcified Tissue International*, 63,
1233 475-481.
- 1234 Posner, A.S. (1985) The mineral of bone. *Clinical Orthopaedics and Related Research*, 87-99.
- 1235 Quelch, K.J., Melick, R.A., and Bingham, P.J. (1983) Chemical composition of human bone.
1236 *Archives of Oral Biology*, 28, 665-674.
- 1237 Rakovan, J. and Pasteris, J.D. (2015) A technological gem: Materials, medical, and
1238 environmental mineralogy of apatite. *Elements*, 11, 195-200.
- 1239 Reid, J.W., Pietak, A., Sayer, M., Dunfield, D., and Smith, T.J.N. (2005) Phase formation and
1240 evolution in the silicon substituted tricalcium phosphate/apatite system. *Biomaterials*, 26, 2887-
1241 2897.
- 1242 Rey, C., Kim, H.-M., and Glimcher, M.J. (1994) Maturation of poorly crystalline synthetic and
1243 biological apatites. In P.W. Brown and B. Constantz, Eds., *Hydroxyapatite and Related*
1244 *Materials*, p. 181-187, CRC Press, Boca Raton.
- 1245 Rey, C., Miquel, J.L., Facchini, L., Legrand, A.P., and Glimcher, M.J. (1995) Hydroxyl groups
1246 in bone mineral. *Bone*, 16, 583-586.
- 1247 Rey, C., Combes, C., Drouet, C., Lebugle, A., Sfihi, H., and Barroug, A. (2007a) Nanocrystalline
1248 apatites in biological systems: Characterisation, structure and properties. *Materialwissenschaft*
1249 *und Werkstofftech*, 38, 996-1002.
- 1250 Rey, C., Combes, C., Drouet, C., Sfihi, H., and Barroug, A. (2007b) Physico-chemical properties
1251 of nanocrystalline apatites: Implications for biominerals and biomaterials. *Materials Science and*
1252 *Engineering C*, 27, 198-205.
- 1253 Rey, C., Combes, C., Drouet, C., and Glimcher, M.J. (2009) Bone mineral: Update on chemical
1254 composition and structure. *Osteoporosis International*, 20, 1013-1021.
- 1255 Reznikov, N., Shahar, R., and Weiner, S. (2014) Bone hierarchical structure in three dimensions.
1256 *Acta Biomaterialia*, 10, 3815-3826.

- 1257 Riboud, P.V. (1973) Composition et stabilite des phases a structure d'apatite dans le systeme
1258 CaO-P₂O₅-oxyde de fer-H₂O a haute temperature. Annales de Chimie (Paris), 8, 381-390.
- 1259 Robinson, R.A. (1955) Crystal-collagen relationships in bone as observed in the electron
1260 microscope. III. Crystal and collagen morphology as a function of age. Annals of the New York
1261 Academy of Sciences, 60, 596-630.
- 1262 Rogers, K. and Zioupos, P. (1999) The bone tissue of the rostrum of a *Mesoplodon densirostris*
1263 whale: A mammalian biomineral demonstrating extreme texture. Journal of Materials Science
1264 Letters, 18, 651-654.
- 1265 Rupani, A., Hidalgo-Bastida, L.A., Rutten, F., Dent, A., Tuner, I., and Cartmell, S. (2012)
1266 Osteoblast activity on carbonated hydroxyapatite. Journal of Biomedical Materials Research Part
1267 A, 100A, 1089-1096.
- 1268 Sahai, N. (2005) Modeling apatite nucleation in the human body and in the geochemical
1269 environment. American Journal of Science, 305, 661-672.
- 1270 Salinas, A.J., Esbrit, P., and Vallet-Regi, M. (2013) A tissue engineering approach based on the
1271 use of bioceramics for bone repair. Biomaterials Science, 1, 40-51.
- 1272 Sepelak, V., Begin-Colin, S., and Le Caer, G. (2012) Transformations in oxides induced by high-
1273 energy ball-milling. Dalton Transactions, 41, 11927-11948.
- 1274 Shepherd, J.H. and Best, S.M. (2011) Calcium phosphate scaffolds for bone repair. JOM, 63, 83-
1275 92.
- 1276 Shi, D. (2006) Introduction to Biomaterials, World Scientific, Singapore.
- 1277 Skinner, H.C.W. (1973) Phase relations in the CaO-P₂O₅-H₂O system from 300 to 600 °C at 2 kb
1278 H₂O pressure. American Journal of Science, 273, 545-560.
- 1279 Skinner, H.C.W. (1987) Bone: Mineralization. In J.A. Albright and R.A. Brand, Eds., The
1280 Scientific Basics of Orthopaedics, p. 199-211, Appleton and Lange Press, Norwalk, CT.
- 1281 Skinner, H.C.W. (2005) Mineralogy of bone. In O. Selinus, B. Alloway, J.A. Centeno, R.B.
1282 Finkelman, R. Fuge, U. Lindh, and P. Smedley, Eds., Essentials of Medical Geology, p. 667-693,
1283 Elsevier, New York.
- 1284 Sprio, S., Tampieri, A., Landi, E., Sandri, M., Martorana, S., Celotti, G., and Logroscino, G.
1285 (2008) Physico-chemical properties and solubility behaviour of multi-substituted hydroxyapatite
1286 powders containing silicon. Materials Science and Engineering C, 28, 179-187.
- 1287 Stevens, M.M. (2008) Biomaterials for bone tissue engineering. Materials Today, 11, 18-25.

- 1288 Suchanek, W.L., Byrappa, K., Shuk, P., Riman, R.E., Janas, V.F., and TenHuisen, K.S. (2004)
1289 Mechanochemical-hydrothermal synthesis of calcium phosphate powders with coupled
1290 magnesium and carbonate substitution. *Journal of Solid State Chemistry*, 177, 793-799.
- 1291 Surmenev, R.A., Surmenev, M.A., and Ivanova, A.A. (2014) Significance of calcium phosphate
1292 coatings for the enhancement of new bone osteogenesis – A review. *Acta Biomaterialia*, 10, 557-
1293 579.
- 1294 Talmage, R.V. and Mobley, H.T. (2009) The concentration of free calcium in plasma is set by
1295 the extracellular action of noncollagenous proteins and hydroxyapatite. *General and Comparative*
1296 *Endocrinology*, 162, 245-250.
- 1297 Tao, J., Battle, K.C., Pan, H., Salter, E.A., Chien, Y.-C., Wierzbicki, A., and De Yoreo, J.J.
1298 (2015) Energetic basis for the molecular-scale organization of bone. *Proceedings of the National*
1299 *Academy of Sciences*, 112, 326-331.
- 1300 Tas, A.C. (2014) The use of physiological solutions or media in calcium phosphate synthesis and
1301 processing. *Acta Biomaterialia*, 10, 1771-1792.
- 1302 Termine, J.D. (1972) Mineral chemistry and skeletal biology. *Clinical Orthopaedics and Related*
1303 *Research*, 85, 207-239.
- 1304 Vandecandelaere, N., Rey, C., and Drouet, C. (2012) Biomimetic apatite-based biomaterials: On
1305 the critical impact of synthesis and post-synthesis parameters. *Journal of Materials Science:*
1306 *Materials in Medicine*, 23, 2593-2606.
- 1307 Veis, A. (1993) Mineral-matrix interactions in bone and dentin. *Journal of Bone and Mineral*
1308 *Research*, 8, S493-S497.
- 1309 Wagermaier, W., Klaushofer, K., and Fratzl, P. (2015) Fragility of bone material controlled by
1310 internal interfaces. *Calcified Tissue International*, 97, 201-212.
- 1311 Weiner, S. and Wagner, H.D. (1998) The material bone: Structure-mechanical function relations.
1312 *Annual Review of Materials Science*, 28, 271-298.
- 1313 Wegst, U.G.K., Bai, H., Saiz, E., Tomsia, A.P., and Ritchie, R.O. (2015) Bioinspired structural
1314 materials. *Nature Materials*, 14, 23-46.
- 1315 White, T., Ferraris, C., Kim, J., and Madhavi, S. (2005) Apatite – An adaptive framework
1316 structure. In G. Ferraris and S. Merlino, Eds., *Micro- and Mesoporous Mineral Phases*, 57, p.
1317 307-401. *Reviews in Mineralogy and Geochemistry*, Mineralogical Society of America,
1318 Chantilly, Virginia.
- 1319 White, A.A., Kinloch, I.A., Windle, A.H., and Best, S.M. (2010) Optimization of the sintering
1320 atmosphere for high-density hydroxyapatite-carbon nanotube composites. *Journal of the Royal*

- 1321 Society Interface, 7, S529-S539.
- 1322 Williams, D.F. (1987) Definitions in Biomaterials: Proceedings of a Consensus Conference of
1323 the European Society for Biomaterials, Chester, England, March 3-5, 1986, Elsevier, New York.
- 1324 Wilson, E.E., Awonusi, A., Morris, M.D., Kohn, D.H., and Tecklenburg, M.M.J. (2006a) Three
1325 structural roles for water in bone observed by solid-state NMR. Biophysical Journal, 90, 3722-
1326 3731.
- 1327 Wilson, R.M., Dowker, S.E.P., and Elliott, J.C. (2006b) Rietveld refinements and spectroscopic
1328 structural studies of a Na-free carbonate apatite made by hydrolysis of monetite. Biomaterials,
1329 27, 4682-4692.
- 1330 Wopenka, B. and Pasteris, J.D. (2005) A mineralogical perspective on the apatite in bone.
1331 Materials Science and Engineering C, 25, 131-143.
- 1332 Xie, B. and Nancollas, G.H. (2010) How to control the size and morphology of apatite
1333 nanocrystals in bone. Proceedings of the National Academy of Sciences, 107, 22369-22370.
- 1334 Yoder, C.H., Pasteris, J.D., Worcester, K.N., and Schermerhorn, D.V. (2012a) Structural water
1335 in carbonated hydroxylapatite and fluorapatite: Confirmation by solid state ²H NMR. Calcified
1336 Tissue International, 90, 60-67.
- 1337 Yoder, C.H., Pasteris, J.D., Worcester, K.N., Schermerhorn, D.V., Sternlieb, M.P., Goldenberg,
1338 J.E., and Wilt, Z.T. (2012b) Dehydration and rehydration of carbonate fluor- and
1339 hydroxylapatite. Minerals, 2, 100-117.
- 1340 Young, R.A. (1975) Biological apatite vs. hydroxyapatite at the atomic level. Clinical
1341 Orthopaedics and Related Research, 113, 249-262.
- 1342 Zipkin, I. (1970) Inorganic composition of bone. In H. Schraer, Ed., Biological Calcification:
1343 Cellular and Molecular Aspects, p. 69-104, Appleton-Century-Crofts, New York.
- 1344
- 1345
- 1346
- 1347
- 1348
- 1349

1350

Figure Captions

1351 **Figure 1.** List of many of the most commonly used biomaterials for replacement or
1352 enhancement of skeletal and other elements of the human body. Adapted and used by
1353 permission of World Scientific, from Hench and Wilson (1993), *An Introduction to Bioceramics*,
1354 Fig. 1, p. 2.

1355

1356 **Figure 2.** Solubility of Ca-P phases at 37 °C in a solution containing equal total molar
1357 concentrations of Ca and P (i.e., T_{Ca} and T_P , respectively) and with an ionic strength of 0.1 mol l⁻¹.
1358 ¹. At pH values above 4, HA is the least soluble, i.e., most stable, Ca-P phase. Modified and
1359 used by permission of Sage Publications, from Johnsson and Nancollas (1992), *Critical Reviews*
1360 *in Oral Biology and Medicine*, vol. 3, Fig. 1, p. 65.

1361

1362 **Figure 3.** Two different representations of the CaO-P₂O₅ binary system, showing that the partial
1363 pressure of water is key to hydroxylapatite stability. The C_xP_y notation indicates the CaO:P₂O₅
1364 molar ratio in the phase; see Table 1 for abbreviations. **(a)** Essentially anhydrous CaO-P₂O₅
1365 binary, on which there is no stability field for HA. Shading indicates the HA-pertinent
1366 compositional region. Adapted and used by permission of the American Chemical Society, from
1367 Kreidler and Hummel (1967), *Inorganic Chemistry*, vol. 6, no. 5, Fig. 3, p. 891. **(b)** Quasi-binary
1368 of the CaO-P₂O₅-(H₂O) system at H₂O partial pressure of 65.5kPa. Adapted and used by
1369 permission of Elsevier, from Riboud (1973), *Annales de Chimie (Paris)*, vol. 8, no. 6, Fig. 3a, p.
1370 384. Shading indicates fields in which HA is stable. Note that the values of phase transition
1371 temperatures T_1 and T_2 depend on the specific water pressure (cf. White et al. 2010). Figures

1372 modified from Heimann and Lehmann (2015, p. 264).

1373

1374 **Figure 4. (a)** The system CaO-P₂O₅-H₂O at 200 °C and 1700 kPa. Adapted and used by
1375 permission of John Wiley and Sons, from Feng and Rockett (1979), Journal of the American
1376 Ceramic Society, vol. 62, Fig. 1, p. 620. The C_xP_y notation indicates the CaO:P₂O₅ molar ratio in
1377 the phase; see Table 1 for abbreviations. Under these conditions, only three solid phases coexist
1378 with aqueous solution, i.e., HA, monetite (DCP, C₂P), and MCPM (CP). In the central 3-phase
1379 field of HA + CaHPO₄ (DCP) + LIQ, two solid phosphate phases coexist together with aqueous
1380 solution. Experiments at lower temperature show brushite (DCPD, C₂P dihydrate) in equilibrium
1381 with solution (Elmore and Farr 1940). Note the narrow width of the HA + LIQ field. **(b)**
1382 Schematic representation of the system CaO-H₃PO₄-H₂O at 25 °C. Adapted and used by
1383 permission of John Wiley and Sons, from Brown (1992), Journal of the American Ceramic
1384 Society, vol. 75, Fig. 3b, p. 19.

1385

1386 **Figure 5.** Analyses of (1) hydroxylapatite standard from the National Institute of Standards and
1387 Technology and (2) cow bone that has been soaked in bleach to remove much of the collagen.
1388 **(a)** X-ray diffractograms. Extreme peak-broadening in (2) indicates a low degree of
1389 crystallinity. Note that all peaks exhibited by the bone apatite can be referenced to those in the
1390 (1) HA standard. **(b)** Infrared spectra. The spectrum of bone apatite (2) displays vibrational
1391 bands for carbonate (C-O) and water (H-O-H), whereas the HA standard (1) shows no
1392 incorporated carbonate, but more hydroxyl (H-O). Adapted and used by permission of John
1393 Wiley and Sons, from LeGeros et al. (2009), Advanced Biomaterials: Fundamentals, Processing,

1394 and Applications, Fig. 2.11, p. 41.

1395

1396 **Figure 6.** FTIR analysis of a synthetic carbonated apatite in the $\nu_4\text{PO}_4$ portion of the spectrum.

1397 The recorded peaks (coarsely dotted traces, in blue on-line, showing the highest absorbance

1398 values) have been deconvolved into their underlying bands, which are shown in narrower vs.

1399 bolder line width for distinction. As labeled, some of the bands reflect features of the apatite

1400 lattice ("apatitic") and others reflect features of ions adsorbed on the crystallites ("non-apatitic").

1401 Adapted and used by permission of Nova Science Publishers, from Eichert et al. (2009),

1402 Nanocrystalline Apatite-Based Biomaterials, Fig. 5, p. 23.

1403

1404

Table 1. Calcium-phosphate (Ca-P) phases of interest in biomaterials

Name(s) and abbreviation(s)	Formula	XI syst, pH stabil.*	Ca/P	Form, Use, Comments
Monocalcium phosph. monohydrate, MCPM or CP	$\text{Ca}(\text{H}_2\text{PO}_4)_2 \cdot \text{H}_2\text{O}$	tricl., 0.0-2.0	0.5	very acidic
Dicalcium phosphate dihydrate, brushite , DCPD or C_2P	$\text{CaHPO}_4 \cdot 2\text{H}_2\text{O}$	mono., 2.0-6.0	1.0	powder
Dicalcium phosphate anhydrous, monetite , DCP or C_2P	CaHPO_4	tricl., Stable > 100°C	1.0	powder
Amorphous calcium phosphate, ACP	$(\text{Ca}, \text{X})_x(\text{PO}_4, \text{Y})_y \cdot n\text{H}_2\text{O}$ X=Mg ²⁺ , Zn ²⁺ , Sn ²⁺ , Al ³⁺ ; Y=CO ₃ ²⁻ , P ₂ O ₇ ⁴⁻	amorph., ~ 5-12	1.3-2.5	powder; always metastable
Octacalcium phosphate, OCP, C_8P_3	$\text{Ca}_8\text{H}_2(\text{PO}_4)_6 \cdot 5\text{H}_2\text{O}$	tricl., 5.5-7.0	1.33	powder
Tricalcium phosphate, α -TCP, β -TCP = whitlockite or C_3P	$\text{Ca}_3(\text{PO}_4)_2$	hex., Not from aq. soln.	1.50	sintered body or powder; bone graft substitute, spinal fusion, orthopedic, dental
Calcium-deficient hydroxylapatite, CDHA or CDA	$\text{Ca}_{10-x}(\text{HPO}_4)_x(\text{PO}_4)_{6-x}(\text{OH})_{2-x}$, 0 < x < 1	6.5-9.5	1.5-1.67	Ca/P depends on pH of precipitating solution
Carbonated hydroxylapatite, CAP	$\text{Ca}_{10-x}(\text{CO}_3)_x(\text{PO}_4)_{6-x}(\text{OH})_{2-x}$, where 0 < x < 2	pH variable	1.67-2.0	powder, sintered body, bone graft substitute; natural bone
Hydroxylapatite , HA or C_{10}P_3	$\text{Ca}_{10}(\text{PO}_4)_6(\text{OH})_2$	hex., 9.5-12	1.67	sintered body (dense or porous), powder, coating, fiber, composite; bone graft subst., see Fig. 1 for uses.
Fluorapatite , FA	$\text{Ca}_{10}(\text{PO}_4)_6\text{F}_2$	hex., 7-12	1.67	powder; dental
Oxyapatite , OA	$\text{Ca}_{10}(\text{PO}_4)_6\text{O}$	hex., NA	1.67	Not stable in aqueous solution.
Tetracalcium phosph. hilgenstockite , TTCP or C_4P	$\text{Ca}_4(\text{PO}_4)_2\text{O}$	mono., NA	2.0	powder; + H ₂ O, rapidly converts to HA; too basic to be implanted <u>alone</u> in body
Biphasic calcium phosphate, BCP	$\text{Ca}_{10}(\text{PO}_4)_6(\text{OH})_2 + \text{CaSO}_4 \cdot 2\text{H}_2\text{O}$	mixed		powder; spinal fusion, bone graft subst., trauma surgery, scaffold, ophthalmic implant

Note: Solubility at 25°C: ACP > DCPD > OCP > β -TCP > CDHA >> HA > FA (LeGeros et al. 2009; Dorozhkin 2012b).

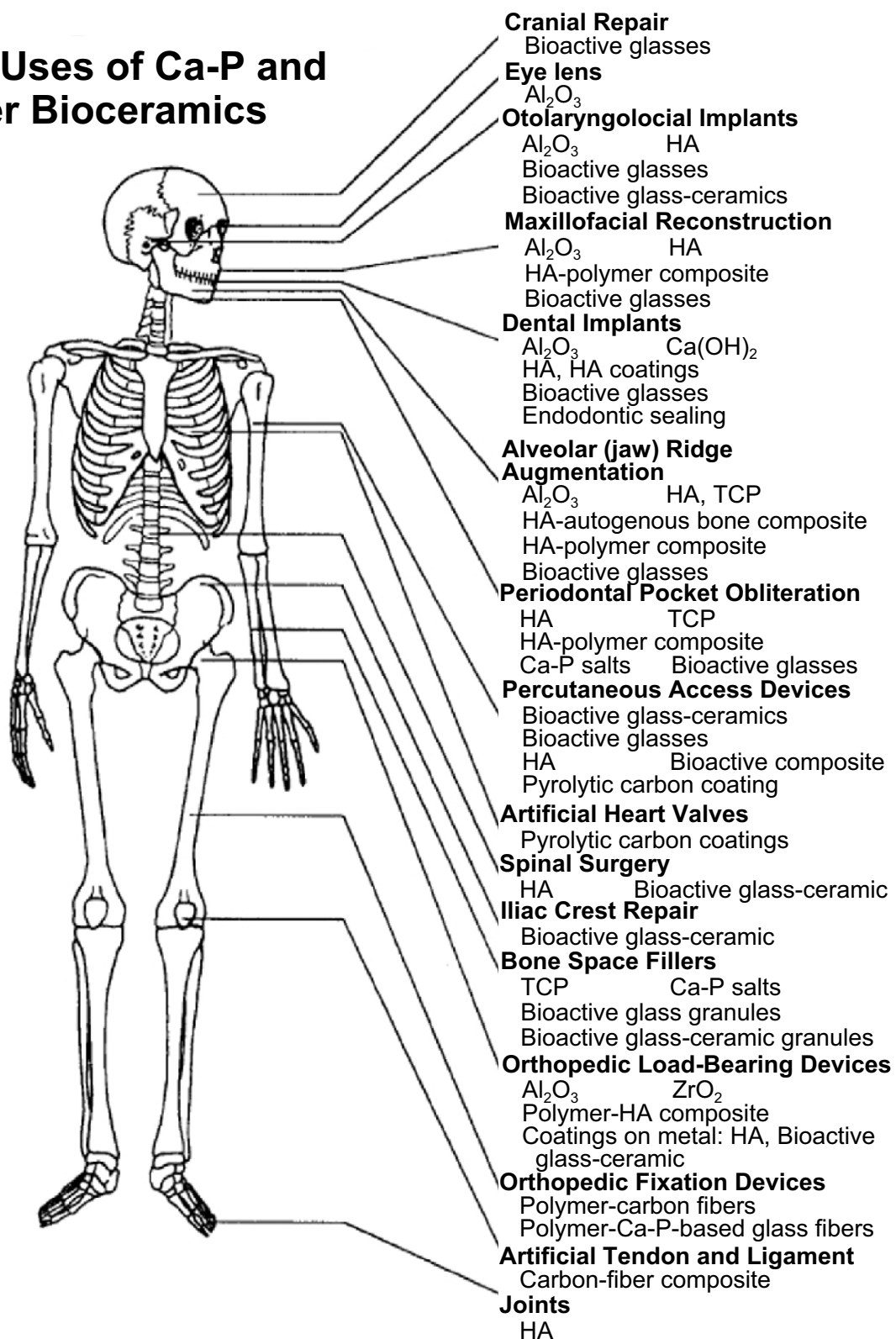
* pH stability range in aqueous solutions at 25 °C. Data from LeGeros et al. (2009), Dorozhkin (2012a,b), and Bayazit et al. (2010).

Table 2. Biomechanical properties of Ca-P and related biomaterials

Material	Young's modulus (GPa)	Compressive strength (MPa)	Fracture toughness (MPa m ^{1/2})
alumina bioceramic	365-400 ^{b,i} (Al ₂ O ₃ 98-99.8%)	1800-4500 ^{b,i}	5-6 ^{b,i}
full sintered zirconia	220 ⁱ		7.4 ⁱ
sintered hydroxylapatite	35-120 ^{c,h,i}	16-145 ^h	1.0 ⁱ
Ca-P cement	30 ^c		
calcium phosphate phases	8-130 ^c		
silicate 13-93 bioglass scaffolds	13 ± 2 ^j	86 ± 9 ^j	
human tooth enamel	9-90 ^{d,i,k}		0.52-1.3
human tooth dentin	11-20 ⁱ , 32.4 ^d		2.8-3.1 ⁱ
cortical bone	7-30 ^{a,b,d,e,h,i,k}	100-250 ^b	2-12 ^{b,k}
trabecular bone	0.05-2.0 ^{b,d,e}	2-12 ^b	
deer and elk antler	wet 6-8 ^{f,g,i} ; dry 7.6 ^f , 17.5 ^g		10.3 ^f [wet, transverse]
collagen	0.6-2 ^{e,k}		
<p><i>Notes:</i> Data from Bonfield et al. (1981)^a, Hench and Wilson (1993)^b, Gross and Berndt (2002)^c, Nath and Basu (2009)^d, Pasteris et al. (2008)^e, Chen et al. (2009)^f, Currey et al. (2009)^g, Dorozhkin (2010)^h, Bayazit et al. (2010)ⁱ, Liu et al. (2013)^j, Wegst et al. (2015)^k.</p>			

Figure 1

Clinical Uses of Ca-P and Other Bioceramics



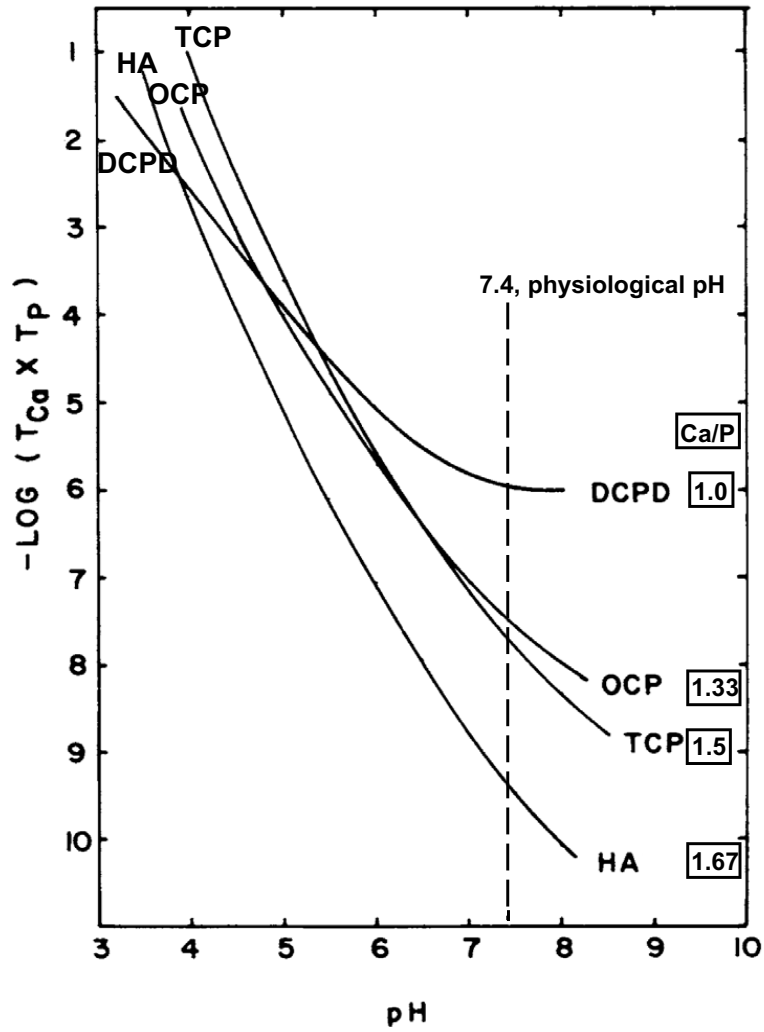
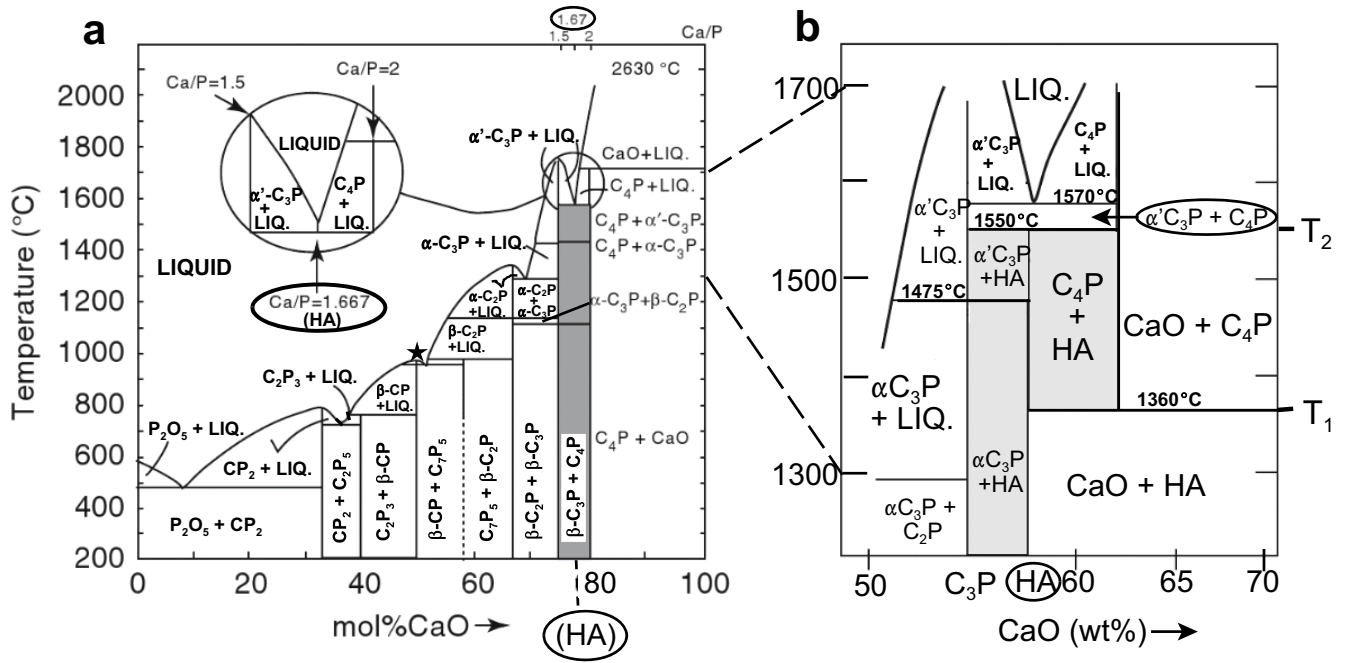


Figure 2

Figure 3



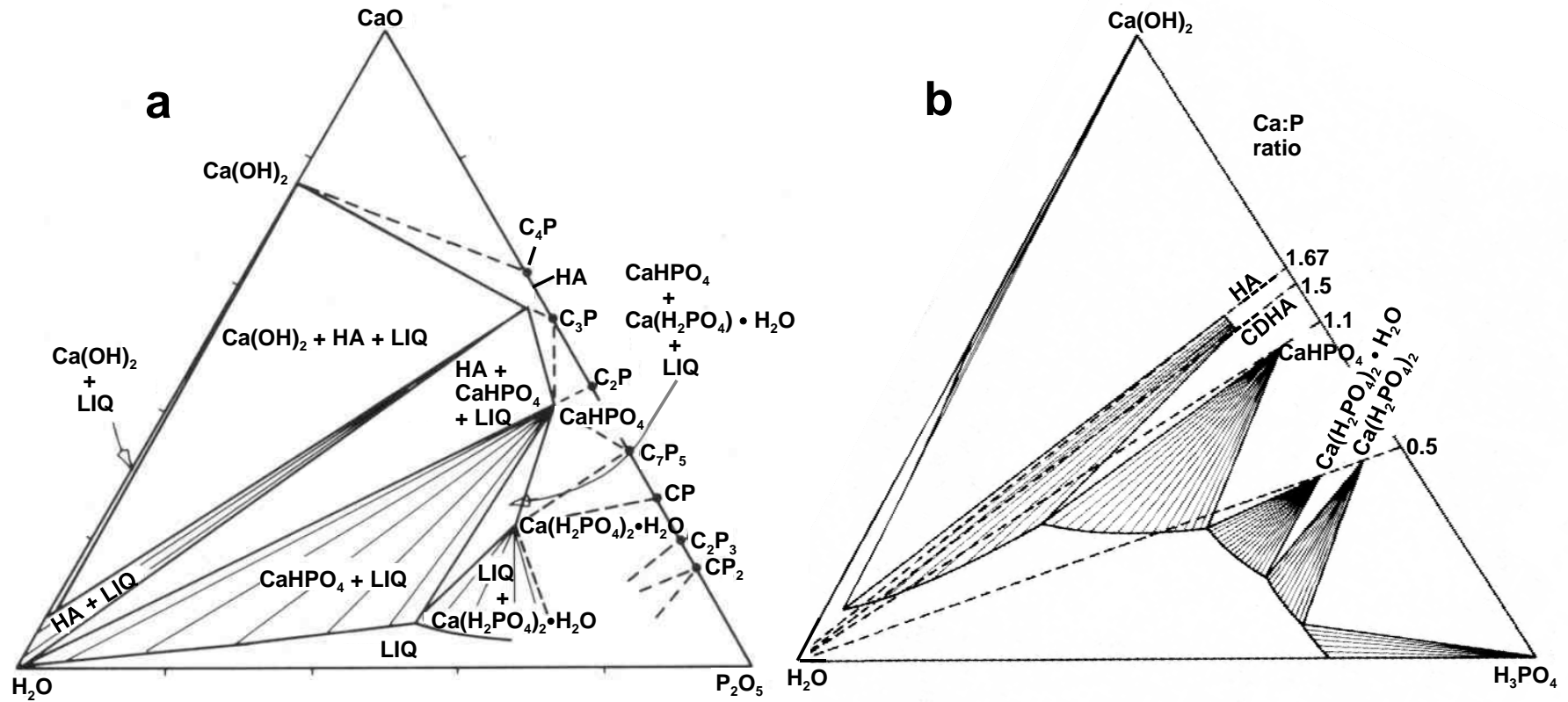


Figure 4

Figure 5

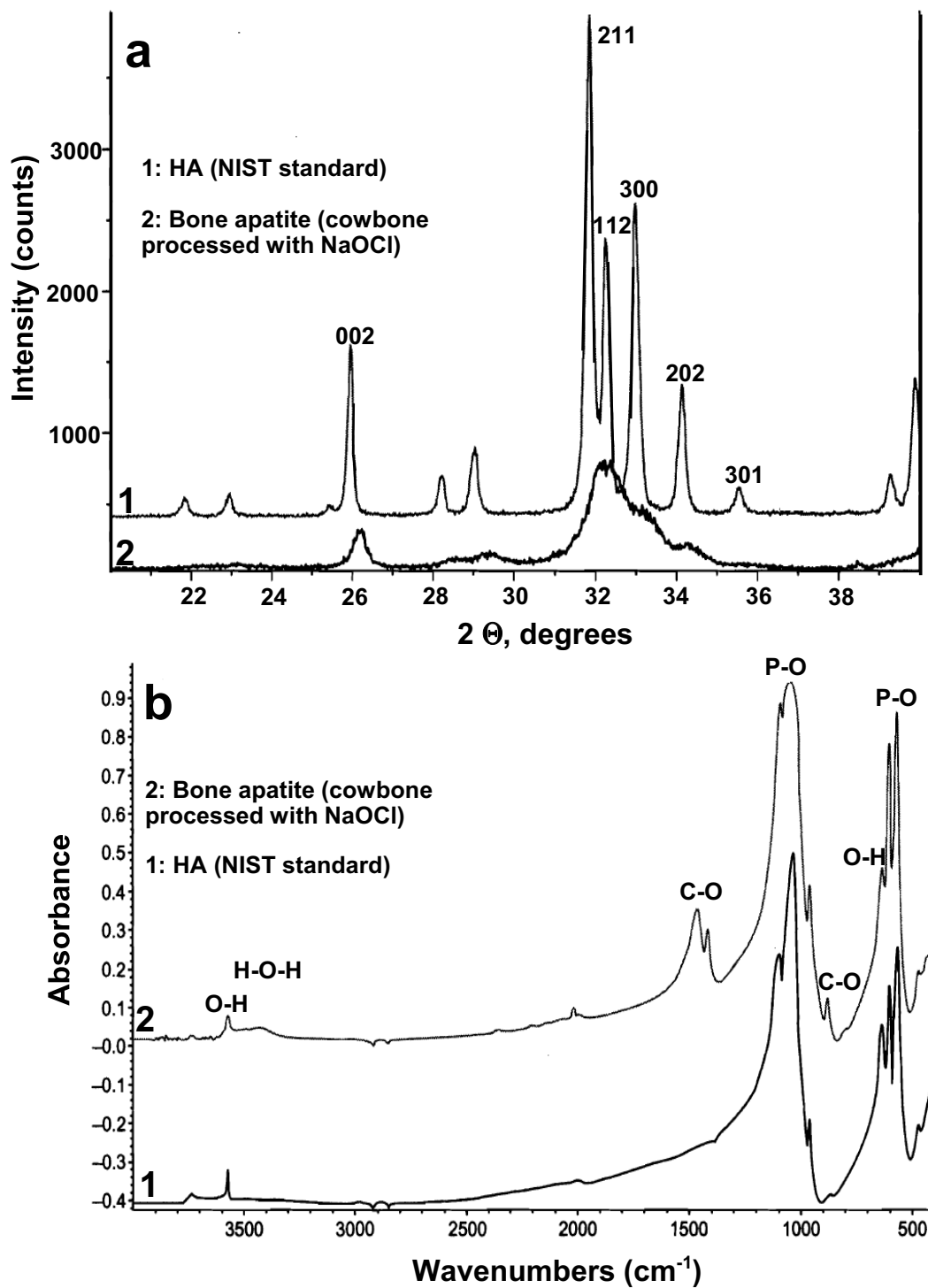


Figure 6

